Journal of Medicinal Chemistry

Freie Universität Berlin

Subscriber access provided by UB + Fachbibliothek Chemie | (FU-Bibliothekssystem)

Article

# Discovery of a highly potent, selective, and metabolically stable inhibitor of receptor-interacting protein 1 (RIP1) for the treatment of systemic inflammatory response syndrome

Yan Ren, Yaning Su, Liming Sun, Sudan He, Lingjun Meng, Daohong Liao, Xiao Liu, Yongfen Ma, Chunyan Liu, Sisi Li, Hanying Ruan, Xiaoguang Lei, Xiaodong Wang, and Zhiyuan Zhang

*J. Med. Chem.*, **Just Accepted Manuscript** • DOI: 10.1021/acs.jmedchem.6b01196 • Publication Date (Web): 19 Dec 2016



ACS Publications

Journal of Medicinal Chemistry is published by the American Chemical Society. 1155 Sixteenth Street N.W., Washington, DC 20036

# Discovery of a highly potent, selective, and metabolically stable inhibitor of receptor-interacting protein 1 (RIP1) for the treatment of systemic inflammatory response syndrome

*Yan Ren*[‡†], *Yaning Su*[‡†], *Liming Sun*[†「], *Sudan He*[†#], *Lingjun Meng*[†], *Daohong Liao*[†], *Xiao Liu*[†], *Yongfen Ma*[†], *Chunyan Liu*[†], *Sisi Li*[†], *Hanying Ruan*[†], *Xiaoguang Lei*[†‖], *Xiaodong Wang*[†*] *and Zhiyuan Zhang*[†§*]

[†]National Institute of Biological Sciences, Beijing 102206, China

[§] Collaborative Innovation Center for Cancer Medicine, Beijing, China

**ABSTRACT**. Based on its essential role in driving inflammation and disease pathology, cell necrosis has gradually been verified as a promising therapeutic target for treating atherosclerosis, systemic inflammatory response syndrome (SIRS), and ischemia injury, among other diseases. Most necrosis inhibitors targeting receptor-interacting protein 1 (RIP1) still require further optimization because of weak potency or poor metabolic stability. We conducted a phenotypic screen and identified a micromolar hit with novel amide structure. Medicinal chemistry efforts

yielded a highly-potent, selective, and metabolically stable drug candidate — compound **56** (RIPA-56). Biochemical studies and molecular docking revealed that RIP1 is the direct target of this new series of type III kinase inhibitors. In the SIRS mice disease model, **56** efficiently reduced tumor necrosis factor alpha (TNFα)-induced mortality and multi-organ damage. Compared to known RIP1 inhibitors, **56** is potent in both human and murine cells, is much more stable *in vivo*, and is efficacious in animal model studies.

## INTRODUCTION

Over the past few decades, necrosis has gradually been verified as an important pathway of programmed cell death, playing essential roles in ovulation,[1] innate immunity,[2] and inflammation[3] in metazoan animals. Programmed cell necrosis is associated with lethal diseases such as ischemia brain/kidney damage, atherosclerosis, myocardial infarction, pancreatitis, and systemic inflammatory response syndrome (SIRS).[4-11] Thus, targeting necrosis pathway can offer a new opportunity for treating these diseases. Three important signaling proteins, receptor-interacting protein 1 (RIP1),[12] receptor-interacting protein 3 (RIP3),[11] and mixed lineage kinase domain-like protein (MLKL),[13] have been recognized as critical components in the regulated necrotic cell death pathway. The identification of the first RIP1 inhibitor — **1** (Necrostatin-1, Nec-1, Figure 1)[7,12] has greatly promoted necrosis pathway research. However, the micromolar potency and poor metabolic stability ($t_{1/2}$ < 5 min) of **1** has limited its application in drug discovery efforts.[14] The most advanced necrostatin reported to date is **2** (Nec-1s)[8] (Figure 1). This compound has better metabolic stability than **1**, but is still only moderately potent, and is difficult to improve structurally, owing to its narrow structure-activity relationship (SAR) profile.

The hybridization of a type-II pan-kinase inhibitor ponatinib with **2** gave compound **3** (PN10)[15] (Figure 1), which had both increased activity and higher kinase selectivity compared to the two compounds upon which it was based. However, the high molecular weight makes **3** unfavorable as a drug and limits its further optimization. The other RIP1 inhibitors listed in Figure 1 were mostly developed by GlaxoSmithKline. The selectivity of **4** (GSK'481)[16] to primate RIP1, the poor pharmacokinetic (PK) stability of **5** (GSK'963),[17] and the poor kinase selectivity profile of **6** (Cpd27)[18] would hinder the development of these compounds as drug candidates. Other known necrosis inhibitors target RIP3 or MLKL (Figure 1). RIP3 inhibitor — **7** (GSK'872),[19] is unsuitable for use as an anti-inflammatory agent because it induces cell apoptosis; the development of **8** (Necrosulfonamide, NSA)[13] as an MLKL inhibitor has been restricted by its moderate anti-necrosis potency and its primate-specific selectivity. Considering the intricately linked involvement of cell necrosis and human diseases, as well as the various limitations of known necrosis inhibitors, the discovery of both novel inhibitors and new protein targets in the necrosis signaling pathway promises to be of significance to both basic biological research and drug discovery.

Necrosomes, which are made up of RIP1, RIP3, and MLKL, induce RIP-kinase activity-dependent necrosis. Treatment of the human colon adenocarcinoma cell line HT29 with a combination of tumor necrosis factor alpha (TNFα), second mitochondrial-derived activator of caspases (Smac) mimetics, and Z-Val-Ala-Asp-(OMe)-Fluoromethyl Ketone (z-VAD-FMK) results in the formation of necrosomes.[3,11] Many biological studies have used TNFα/Smac mimetic/z-VAD-FMK (TSZ)-induced HT29 cell necrosis assays;[11,13,16] indeed the very discovery of the critical role that MLKL plays in the necrosis pathway was based on a screening hit from such assays.[13] Here, we report the discovery of a new series of inhibitors identified from their

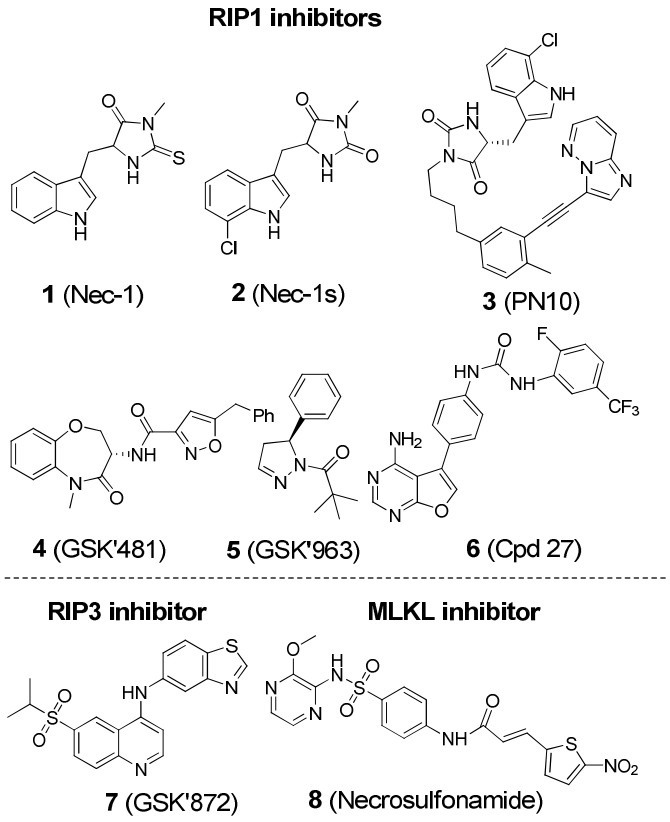


**Figure 1**. Chemical structures of known necrosis inhibitors targeting RIP1, RIP3, and MLKL.

ability to block necrosis in the TSZ-HT29 assay. Our lead-optimization improved the activity of the initial hit compound 340-fold ($EC_{50}$ from 4.1 μM to 12 nM). We subsequently identified and biochemically characterized RIP1 as the cellular target of this new series of type III kinase inhibitors. The highly potent and selective lead compound, N-benzyl-N-hydroxy-2,2-dimethylbutanamide **56** (RIPA-56), showed an impressive PK profile in mice, with a 3.1 h half-life and efficient protection of mice from TNFα-induced mortality and multi-organ damage in the SIRS disease model. Compared to known RIP1 inhibitors, **56** is potent in both human and murine cells, has the best PK profile, and is efficacious in animal model studies*;* thus **56** is a favorable tool compound for studies in animal disease models, and is a potential drug candidate for clinical trials of necrosis-related diseases.

## RESULTS and DISCUSSION

**Discovery of novel anti-necrosis small molecules.** To identify new necrosis inhibitors, a robust TSZ-induced HT-29 cell necrosis assay[11,13] was conducted to screen a chemical library of 200,000 compounds. Hit compound **9** (Figure 2A) was confirmed to block necrotic cell death with an $EC_{50}$ of 4.1 μM; albeit less potent than **1**, but compound **9** still offered a novel core for structural optimization (Figure 2B).

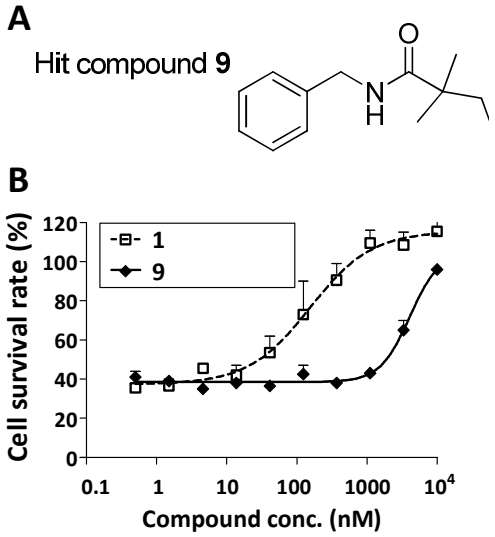


**Figure 2.** Characterization of hit compound **9**. A, Chemical structure of hit compound **9**. B, Protection of **1** and **9** against TSZ-induced HT-29 cell necrosis.

**From hit to lead optimization.** According to the structural features of the initial hit compound **9**, we designed modifications of the compound at its various positions (Table 1) with the goal of improving its potency. We first examined the influences of various substituents on the phenyl ring and the nitrogen of the amide group of hit compound **9** on anti-necrosis potency. Compounds modified from **9** were synthesized, and their inhibition potency was measured *in vitro* using a TSZ-induced HT-29 cell necrosis assay. Introduction of a fluoro group to the 2-

position of the phenyl ring resulted in an approximately 5-fold improvement in anti-necrosis potency (Table 1, **10** vs **9**), while a larger group (*e.g.*, bromine) substituted at both the 2- and 3-positions resulted in dramatically decreased anti-necrosis potency (**11** and **12**). We next turned our efforts to modifications at the nitrogen of the amide. Methylation (**13** and **14**) significantly improved the potency by approximately 10~40-fold, while ethylation (**15**) caused a complete loss of potency, indicating a limited space for further modification at this position. Next, the SAR around the phenyl group was explored by keeping the methyl group on the nitrogen constant and substituting the phenyl ring. Replacement of the fluoro group in the 2-position of the phenyl ring with a chloro group (**16**) caused complete loss of anti-necrosis potency. The 3-fluorine substituted compound **17** improved the potency ($EC_{50}$ = 72 nM), however no improvements were observed for the 3-chlorine substituted compound **18** or the 3-bromine substituted compound **19** or the 4-fluorine substituted compound **21**, and a hydroxyl group at the 3-position of the phenyl ring (**20**) resulted in a complete loss of potency. Encouraged by these results, we further synthesized di-substituted compounds **22-24**. While the $EC_{50}$ values of 2,3-di-F compound **22** and 2,5-di-F compound **24** were further reduced to 58 nM and 36 nM, respectively, the $EC_{50}$ value of 2,4-di-F compound **23** was reduced to 626 nM. These SAR results indicated that substitution with fluorine at the 2-, 3-, or 5-position increased potency and further suggested that larger substitutions at these positions were detrimental to potency. As expected, the 2,3,5- trifluoro substituted derivative (**25**) had yet further improved potency ($EC_{50}$ = 12 nM). In the contrary, the 2,4,6-tri-F compound **26** exhibited much weaker anti-necrosis potency than **25**. Our SAR results suggested that the phenyl ring likely interacts with a tigh hydrophobic pocket of putative target protein.

**Table 1.** SAR study of compounds **9**–**26** evaluated with a TSZ-induced HT-29 cell necrosis assay.

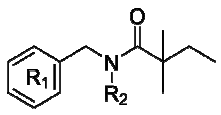


| Compd | $R_1$ | $R_2$ | $EC_{50}$ (nM)[a] | Compd | $R_1$ | $R_2$ | $EC_{50}$ (nM)[a] |
|---|---|---|---|---|---|---|---|
| **9** | phenyl | H | 4100 ± 952 | **18** | 3-Cl-phenyl | Me | 628 ± 94 |
| **10** | 2-F-phenyl | H | 898 ± 48 | **19** | 3-Br-phenyl | Me | 1233 ± 102 |
| **11** | 2-Br-phenyl | H | 8562 ± 869 | **20** | 3-OH-phenyl | Me | > 3000 |
| **12** | 3-Br-phenyl | H | > 10,000 | **21** | 4-F-phenyl | Me | 815 ± 32 |
| **13** | phenyl | Me | 457 ± 53 | **22** | 2, 3-di-F-phenyl | Me | 58 ± 7 |
| **14** | 2-F-phenyl | Me | 125 ± 4 | **23** | 2, 4-di-F-phenyl | Me | 627 ± 1 |
| **15** | 2-F-phenyl | Et | > 10,000 | **24** | 2, 5-di-F-phenyl | Me | 36 ± 7 |
| **16** | 2-Cl-phenyl | Me | > 10,000 | **25** | 2, 3, 5-tri-F -phenyl | Me | 12 ± 2 |
| **17** | 3-F-phenyl | Me | 72 ± 9 | **26** | 2, 4, 6-tri-F-phenyl | Me | 1254 ± 174 |

[a]$EC_{50}$ data of each compound were determined in 2~3 independent assays, and mean $EC_{50}$ ± SD values are shown in the table. Compd: abbreviation of compound; SD: standard deviation. These data formats and abbreviations are used in the tables that follow.

In order to further explore SAR of hit compound **9**, we investigated replacement of the phenyl ring with heterocyclic analogs (Table 2). Substitution of this moiety with pyridine derivatives (*e.g.* compounds **27** and **29**) resulted in a complete loss of potency. Compound **28** also had greatly reduced potency in comparison with compound **13**. In contrast, replacement of the phenyl ring with a thiophene moiety increased activity 2-fold (**30** vs **13**), while compound **32** had a similar potency as **13**. Compounds **31** and **33** displayed weaker anti-necrosis potency with $EC_{50}$ values in the range of 1 - 3 μM. Compound **34**, which has a furan group in place of the phenyl ring had slightly lower activity than compound **13**, while derivatives carrying either 2-methylthiazole (**35**) or 1-methyl-1H-pyrazole (**36**) groups lost all anti-necrosis potency.

**Table 2.** SAR of N-heterocycle substituted-N,2,2-trimethylbutanamide series **27**–**36**

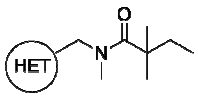


| Compd | HET | $EC_{50}$ (nM) | Compd | HET | $EC_{50}$ (nM) |
|---|---|---|---|---|---|
| **27** |  | > 10,000 | **32** | 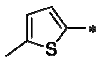 | 378 ± 4 |
| **28** |  | 1735 ± 140 | **33** | 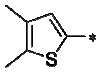 | 1308 ± 81 |
| **29** |  | > 10,000 | **34** |  | 628 ± 72 |
| **30** |  | 221 ± 26 | **35** | 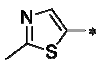 | > 10,000 |
| **31** |  | 2527 ± 227 | **36** | 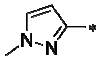 | > 10,000 |

We also investigated the SAR involving the acyl group of compound **9.** First, the original acyl group was substituted with different branched alkylacyl groups. As shown in Table 3, the corresponding region of the binding pocket appeared sensitive to both the size (compounds **37**

and **40**–**44**) and polarity (compounds **38** and **39**), of the substituted acyl groups. Among these, compound **37** showed an $EC_{50}$ of 97 nM, approximately 8-fold less potent than its parent, compound **25**. The introduction of hydroxyl and methoxyl groups, as in compounds **38** and **39**, caused complete loss of activity. Cyclic analogs of these compounds (**40**–**44**) all showed a dramatic loss of activity. Replacement of the amide moiety with urea also impaired the anti-necrosis potency; compounds **45**–**48** showed greatly weak potency compared to the amide compound **25**. Overall, the 2,2-dimethylbutanamide moiety was shown to be the most effective acyl group within this class of compounds for high levels of anti-necrosis potency.

**Table 3.** SAR of acyl group replacement (compounds **37**–**48**)

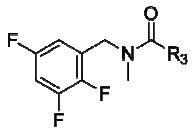


| Compd | $R_3$ | $EC_{50}$ (nM) | Compd | $R_3$ | $EC_{50}$ (nM) |
|---|---|---|---|---|---|
| **37** |  | 98 ± 10 | **43** |  | 1234 ± 200 |
| **38** |  | > 10,000 | **44** |  | 490 ± 86 |
| **39** |  | > 3000 | **45** |  | > 3,000 |
| **40** |  | > 10,000 | **46** |  | > 3000 |
| **41** |  | 8237 ± 1180 | **47** |  | > 3,000 |
| **42** |  | 656 ± 60 | **48** |  | 1526 ± 204 |

We also examined the influence of $R_4$ substitution on compound **9** (Table 4). Substitution of the $R_4$ group with a methyl group, $-(CH_3)_2$ and $-CH_2CH_2-$ group, as in compounds **49**, **52**, and **54,** respectively, caused inactivation (Table 4). Addition of a methyl group to the amide nitrogen of compounds **49** and **52**, to produce compounds **50** and **55**, respectively, did not improve the inhibitory potency of either original compound. Introduction of a hydroxymethyl group to compound **9** (compound **51)** increased potency by ~4-fold relative to the original. However, methylation of compound **51** nitrogen atom, to form compound **53**, did not increase potency. The results suggested that there is no more room for further SAR study at this area.

**Table 4.** SAR of compound **49**–**55**.

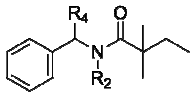


| Compd | $R_2$ | $R_4$ | $EC_{50}$ (nM) |
|---|---|---|---|
| **49** | H | Me | > 10,000 |
| **50** | Me | Me | > 10,000 |
| **51** | H | $-CH_2OH$ | 1077 ± 124 |
| **52** | H | $-(CH_3)_2$ | > 10,000 |
| **53** | Me | $-CH_2OH$ | > 10,000 |
| **54** | H | $-CH_2CH_2-$ | > 5,000 |
| **55** | Me | $-(CH_3)_2$ | > 10,000 |

Using the results of our SAR studies, a 340-fold increase in bioactivity from $EC_{50}$ of 4.1 μM for compound **9** to 12 nM for compound **25**, we expanded our optimization study to produce derivatives with increased stability. We selected a sub-set of potent compounds for *in vitro* microsomal stability assays using human and mouse liver microsomes. The stability of most N-methylated compounds was low in both types of liver microsomes ($t_{1/2}$ less than 5 min, Table s1). In contrast, compounds **9**, **49** and **51** had higher microsomal stability ($t_{1/2}$ > 200 min, Table s1) in human liver microsomes. Although none of the three compounds had a high potency (Tables 1 and 4), the additional polar groups (OH or NH) possibly contributed to their stability. Following these results, we synthesized a subsequent set of N-hydroxylated compounds (**56**–**62**) (Table 5). These compounds were tested for cell necrosis inhibition, yielding results comparable to the SAR of N-methylated compounds. Notably, compound **56** had a half-life of 128 min in human liver microsomal stability assays and an $EC_{50}$ of 28 nM in TSZ-induced HT-29 necrosis assay. Compound **56** also demonstrated potency in protection of murine L929 cells from TZ-induced necrosis ($EC_{50}$ = 27 nM, Figure s1). This result is ~100-fold more potent than GSK benzoxazepinone compound **4** (Figure 1),[16] which has higher activity in primate, rather than non-primate, RIP1. We conclude from these stability and activity data that compound **56** is well-suited as a lead for further study in the mouse model.

**Identification of RIP1 as the direct target of the amide series of necrosis inhibitors.** As this is a novel series of necrosis inhibitors, we wanted to know if they target RIP1, RIP3, MLKL or an unknown target associated with this necrosis pathway. It is known RIP1 and RIP3 are phosphorylated following TSZ treatment; this phosphorylation can be monitored as up-shifted bands as detected via western blotting. The phosphorylation level of RIP3 is known to depend on both its own kinase activity and the kinase activity of RIP1.[11] According to the band shift results

**Table 5.** SAR and liver metabolic stability of N-OH compounds **56**–**62**.

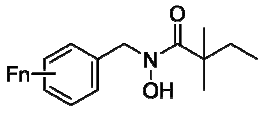


| Compd | Fn | $EC_{50}$ (nM) | Human Liver Microsomes | | Mouse Liver Microsomes | |
|---|---|---|---|---|---|---|
| | | | $t_{1/2}$ (min) | Clint (μL/min/mg) | $t_{1/2}$ (min) | Clint (μL/min/mg) |
| **56** | - | 28 ± 3 | 128 | 5.40 | 35.5 | 19.5 |
| **57** | 4-F | 64 ± 11 | 178 | 3.90 | 24.1 | 28.8 |
| **58** | 2, 4-di-F | 198 ± 36 | 198 | 3.50 | 23.2 | 29.9 |
| **59** | 3, 4-di-F | 56 ± 4 | 107 | 6.50 | 11.3 | 61.4 |
| **60** | 2, 3,4-tri-F | 262 ± 28 | 52.9 | 13.1 | 13.9 | 49.9 |
| **61** | 3, 4,5-tri-F | 49 ± 5 | 66.0 | 10.5 | 7.89 | 87.8 |
| **62** | 2, 3,5-tri-F | 74 ± 17 | 66.6 | 10.4 | 9.21 | 75.3 |

shown in Figure 3A, **56** can block the phosphorylation of both RIP1 and RIP3. The **56**-mediated inhibition was confirmed using an antibody specific for phosphorylation on Serine227 of RIP3. **56** thus appears to inhibit the kinase activity of RIP1 and/or RIP3, or to somehow interfere with their upstream activators. The kinase activities of RIP1 and RIP3 were next monitored *in vitro*

using an ADP-Glo assay.[15] Compound **56** showed efficient inhibition of RIP1 kinase activity, with an $IC_{50}$ of 13 nM (Figure 3B), 57-fold more potent than **1** ($IC_{50}$ = 760 nM).[15] It showed no inhibition of RIP3 kinase activity at a 10 μM concentration (Figure s2A). Several new compounds were evaluated using this RIP1 kinase activity assay. A good correlation was noted between kinase inhibition activity data and cell necrosis inhibition data (Figure s2B), indicating that RIP1 is the direct target of these new amide series inhibitors.

According to a reported complex structure of RIP1-Nec1,[20] an allosteric back-pocket is isolated from its ATP binding site and forms an L-shaped hydrophobic pocket. This pocket is divided into two parts by phenylalanine (Phe)-162. Our molecular docking simulation study suggested that compound **56** fits tightly in this pocket, similar to **1** (Figure 3C). This binding mode implies the existence of a key hydrogen bond that is formed between the carbonyl group on the inhibitor molecule and the NH of aspartic acid (Asp)-156 of RIP1. The phenyl group occupies the left side of the pocket formed by leucine (Leu)-70, Leu-129, valine (Val)-134, histidine (His)-136, isoleucine (Ile)-154, and serine (Ser)-161, and it seems likely that this narrow space would not tolerate larger substituents on the phenyl ring or polar hetero aromatic ring, which is consistent with our SAR results reported in Tables 1 and 2. On the right side of the pocket, only the 2,2-dimethylbutanamide moiety could effectively occupy the hydrophobic pocket space; both the presence of one additional carbon and the absence of one of these carbons resulted in a dramatic decrease in potency (Table 3). Furthermore, inefficient and unsuitable occupancy in this area by various urea analogs from our SAR studies seems likely to be a major factor contributing to activity loss. For the N-OH compounds, the hydroxyl group may also form a hydrogen bond with valine (Val)-76, which could explain the slight SAR changes among the phenyl substitutions shown in Table 5. Furthermore, this proposed binding mode for the

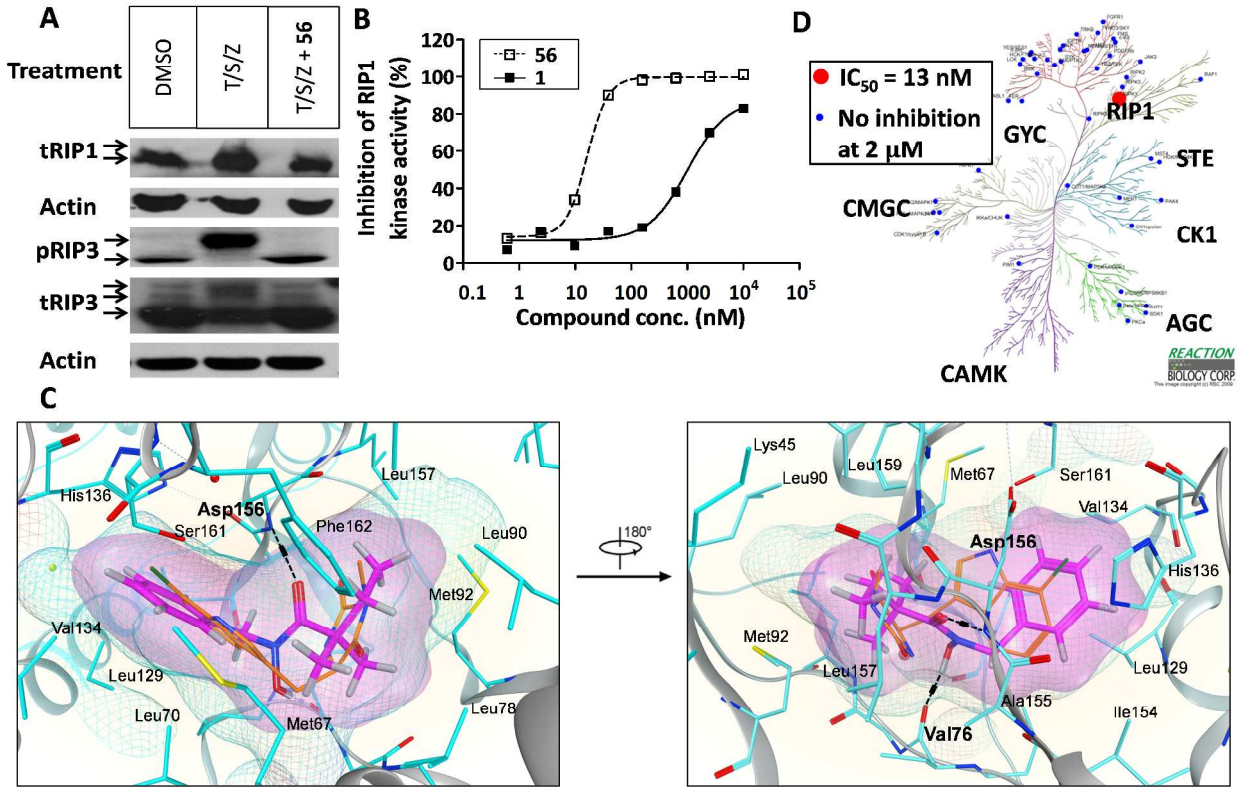


**Figure 3**. Target validation and kinase panel screening of lead compound **56**. A, compound **56** inhibits TSZ-induced phosphorylation of RIP1 and RIP3 in HT-29 cells. B, Compound **56** is more potent than **1** in inhibiting RIP1 kinase activity. C, Based on the molecular docking simulation study, compound **56** could form tight hydrophobic interactions with RIP1 through both the phenyl group and the 2,2-dimethylbutyl group, and form two important hydrogen bonds (one between the carbonyl oxygen of **56** and the backbone NH on Asp156 of RIP1, the other occurs between the N-OH of **56** and Val76 of RIP1). D, compound **56** shows good selectivity in kinase panel screening (conducted by Reaction Biology Corp.)

inhibitors suggests that the compounds are likely type III kinase inhibitors that lock the RIP1 kinase in its inactive form. This would be in line with its absolute selectivity according to the kinase panel screening results (Figure 3D, Figure s2C). Compound **56** was also tested in IDO

enzyme activity assays. Unlike **1**,[8, 21, 22] **56** did not inhibit IDO activity at a concentration of 200 μM, which represents an estimated 10,000-fold selectivity window based on the RIP1 ADP-Glo activity of 13 nM; **56** therefore avoids the problematic off-target (anti-IDO) effect of **1** (Figure s3).

**Pharmacokinetics and pharmacological efficacy of** 56 ***in vivo*.** We conducted metabolic stability assays and noted that **56** had a marked improvement in liver microsomes (Table 5). **56** also had an impressive PK profile in mice (Table s2, Figure 4), with a 3.1 h half-life, 22% oral bioavailability (PO), and 100% bioavailability from intraperitoneal injection (IP). Encouraged by its high potency and high selectivity in biochemical and cellular studies, and good metabolic stability in these *in vivo* PK studies, we were also interested to see whether **56** could confer any therapeutic effect in mice models of inflammatory diseases.

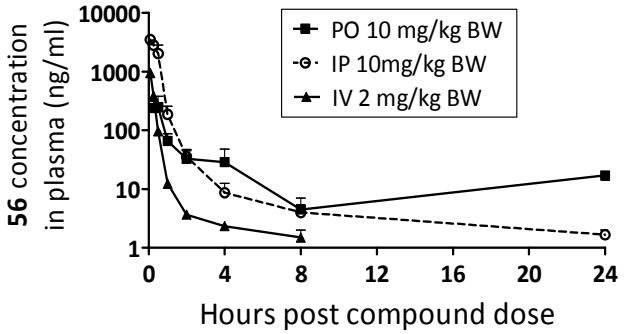


**Figure 4.** Pharmacokinetics of oral (PO), intraperitoneal (IP), and intravenous (IV) administration of **56** in C57BL/6 mice (n = 3; BW: body weight).

TNFα administration can cause multiple organ dysfunction and death in mice, exhibiting many similarities with the highly-lethal human SIRS disorder that can be induced by infection, trauma, etc.[4,6,8,15-17] To test whether **56** has any efficacy in protecting against TNFα-induced lethality, 5.5 μg of mouse TNFα (mTNFα) (~0.25 mg/kg body weight (BW)) was intravenously injected to

C57BL/6 mice (6-8 weeks, 20-25 g) and mice were either treated with multiple-dose of **56** (0.1, 1, 3 mg/kg BW, IP, 17 min before mTNFα injection and once every 12 h) or a single dose of **56** or **1** (6 mg/kg BW, IP, 17 min before mTNFα injection). As shown in Figure 5, both multiple-dose and single-dose of **56** treatment dramatically increased the survival rate of TNFα-treated mice, showing a dose-dependent effect. Mice treated with multiple-dose of **56** (3 mg/kg) or a single 6 mg/kg dose of **56** had a survival rate of 100%, much higher than the TNFα/**1** group, which had a survival rate of 60%. The TNFα/vehicle-treated mice group had a 50% survival rate.

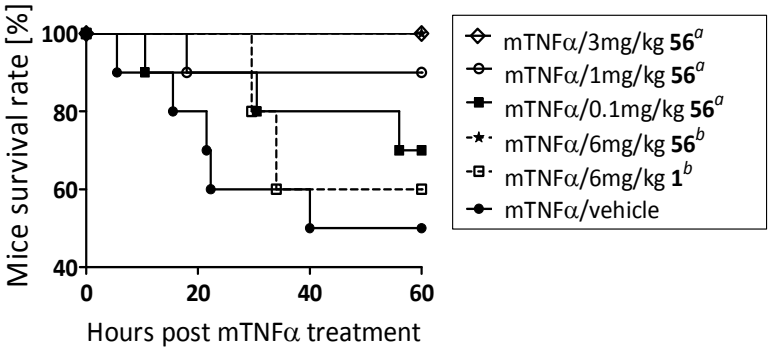


**Figure 5.** Both multiple dose of **56** (0.1, 1, 3 mg/kg BW, IP, once every 12 h) and a single dose of **56** (6 mg/kg BW, IP, once) can protect mice from mTNFα-induce death (n = 6~10 per group). This protection was significantly better than that conferred by a single 6 mg/kg BW dose of **1**. [a]multiple-dose; [b]single dose.

To test the efficacy of **56** in protecting against TNFα-induced multi-organ damage, 4 μg mouse TNFα (mTNFα) (~0.18 mg/kg BW) was intravenously injected into C57BL/6 mice. The levels of the mouse pro-inflammatory cytokines interleukin-6 (mIL-6) and interleukin-1ß (mIL-1ß) increased significantly after TNFα induction, but mice treated with **56** had lower or even normal levels of cytokines (Figure 6A). Note that mice treated with a single 6 mg/kg dose of **1** had partially-decreased levels of mIL-6 and mIL-1ß (Figure s4), a finding consistant with the

reported protection effects of **1** on mice viability. Histological examination of haematoxylin-eosin (H&E) stained spleens of TNFα-treated mice showed that both the red pulp and the white pulp were infiltrated with many immune cells and macrophages; this pattern was also seen in the cortex and medulla of the thymus (Figure 6B).The thickness of the periarteral lymphatic sheath (PALS) also increased dramatically in TNFα-treated mice. In contrast, the spleen and thymus of mice that were additinally treated with **56** were infiltrated with only a few immune cells and macrophages, and otherwise appeared similar to those of non-TNFα treated control mice. In addition to the immune organs (spleen and thymus), we also examined TNFα-induced damage to other internal organs, including the myocardium, kidneys, and pancreas. For TNFα-treated mice, the level of representive biomarkers, including serum lactate dehydrogenase (LDH), creatine kinase (CK), aspartate aminotransferase (AST), creatinine, blood urea nitrogen (BUN), and amylase, increased by 2 to 10-fold as compared with control mice. Organ damage could also be clearly interpreted from histological staining results, which exhibited infiltration of inflammatory cells, disordered tissues, and damaged cells. In contrast, the biomarker levels of TNFα-treated mice that were also given **56** were close to those of healthy animals, and the extent of organ damage in **56**-treated was limited compared to the TNFα-treated mice (Figure 6).

**Assessment of** 56 **as a drug candidate for clinical trials.** The drug-like properties of **56** were further evaluated. **56** was tested for its ability to inhibit cytochrome P450 enzymes; it had $IC_{50}$ values higher than 50 μM against CYP1A2, 2C19, 2C9, and 2D6, and higher than 3.5 μM against CYP3A4. In addition, a tissue-distribution study indicated that **56** could be delivered readily to most organs where diseases might occur (Figure s5). For example, **56** could be detected in the brains of mice following intravenous injection, and exhibited strong permeability in MDCK-MDR1 cells ($P_{app}$, A-B and B-A > $30 \times 10^6$ cm/sec), with an efflux ratio of 0.87

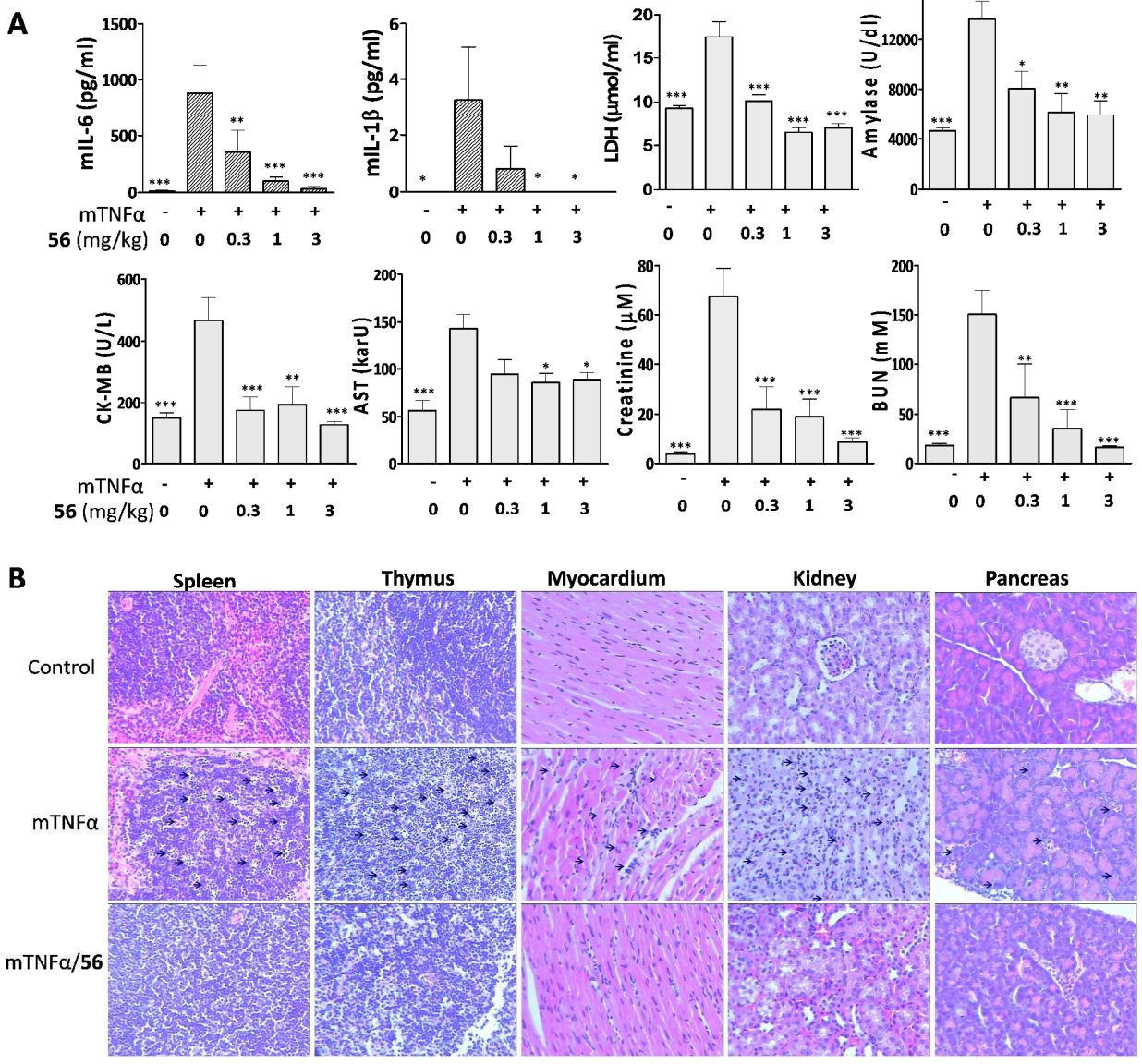


**Figure 6.** **56** can efficiently protect mice from mTNFα-induced multi-organ damage. A, **56** administration (0.3, 1, 3 mg/kg BW, IP, once every 12 h) can decrease the secretion of pro-inflammatory cytokines and level of tissue damage biomarkers. B, **56** shows efficient protection against TNFα-induced injury of different organs. (H&E staining, magnification: ×200). Each image is representative of at least three mice. $^{*}$ $P < 0.05$, $^{**}$ $P < 0.01$, $^{***}$ $P < 0.001$, each vs. TNFα model group.

(Table s3), showing great ability in transporting across blood brain barrier. This is attractive when considering the requirements of therapies against neurodegenerative disease and in treatment of ischemic or traumatic brain injuries, in that **56** could be administrated by IV or IP injection rather than through intracerebroventricular administration. Manual patch clamp evaluation of **56** demonstrated that it did not inhibit the hERG channel, even at concentrations as high as 30 μM (conducted by WuXi AppTec). Multiple-, high-strength dose of **56** (50 mg/kg, once every 3 h, for 24 h) caused no injury to mice. These results from both *in vitro* and *in vivo* studies all indicate that **56** seems to be a safe and potentially efficacious candidate drug for the treatment of necrosis-related diseases.

**Chemistry.** Compounds **10**–**15** were synthesized by a route as shown in Scheme 1. The syntheses began with acylation reaction of corresponding halogen substituted phenylamines with 2, 2-dimethylbutanoyl chloride to obtain compound **10**–**13**, and compound **14** and **15** were obtained through alkylation of **10** with methyl iodide and bromoethane in good yield.

**Scheme 1**. Synthesis of compounds **10**–**15**.

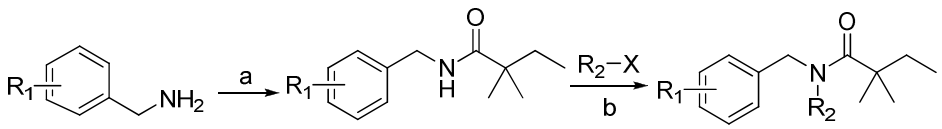


**10**: $R_1$= 2-F **12**: $R_1$=3-Br **14**: $R_1$ = 2-F, $R_2$ = Me
**11**: $R_1$= 2-Br **13**: $R_1$= no substituent **15**: $R_1$ = 2-F, $R_2$= Et

Reagent and conditions: (a) 2, 2-dimethylbutanoyl chloride, TEA, DCM, rt; (b) NaH, R-Br, rt, THF.

Compounds **16**–**48** were prepared according to Scheme 2. Reductive amination of aromatic aldehydes with methylamine using $NaBH_4$ afforded benzylmethylamine compounds, followed by acylation with 2,2-dimethylbutanoyl chloride and different alkyl acid to yield the corresponding

compounds **16**–**36** and **37**–**44**. The urea compounds **45**–**48** were prepared by treatment of the benzylmethylamine intermediates with triphosgene and different alkylamines.

**Scheme 2.** Synthesis of compounds **16**–**48**.

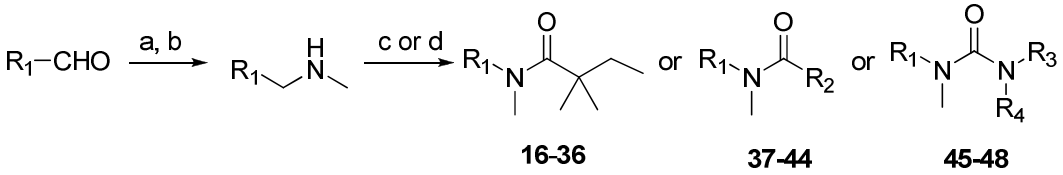


$R_1$ group represented substituent aromatic rings such as benzene, pyridine, and thiophene rings, etc. $R_2$ group represented branched or cyclic alkyl group; $R_3$ and $R_4$ represted hydrogen atom or alkyl group. Reagent and conditions: (a) $CH_3NH_2$, HCl, $K_2CO_3$, MeOH, rt, 1.5 h; (b) $NaBH_4$, rt, 16 h; (c) 2, 2-dimethylbutanoyl chloride, DIEA, THF or DCM, rt, 2 h (for **16**–**36**); (d) $R_2COOH$, HATU, DIEA, DMF, rt, 16 h (for **37**–**44**); (d) $NR_3R_4$, triphosgene, DCM (for **45**–**48**).

The branched benzyl compounds **49**–**55** were synthesized by two routes (Scheme 3). Starting from 1-phenylethan-1-amine **63**, 2-phenylpropan-2-amine **65**, and cyclopropyl(phenyl) methanamine **66**, acylation with 2,2-dimethylbutanoyl chloride gave compounds **49**, **52**, and **54** respectively. Compound **49** and **52** were further methylated with methyl iodide in presence of sodium hydride to give desired products **50** and **55** (Scheme 3A). Compound **51** was obtained by selective amide formation by individually treating N-benzylhydroxylamine **64** with 2,2-dimethylbutanoyl chloride in a mixture of aqueous $NaHCO_3$ and tetrahydrofuran.

Compound **53** was synthesized in three steps as illustrated in Scheme 3B. A commercial available material, 2-amino-2-phenylethan-1-ol **64**, was treated with methyl carbonochloridate to give intermediate **67** that was converted to N-methyl compound **68** by a reduction using $LiAlH_4$, followed by a standard acylation with 2,2-dimethylbutanoyl chloride afforded the desired product **53**.

**Scheme 3.** Synthesis of compounds **49**–**55**.

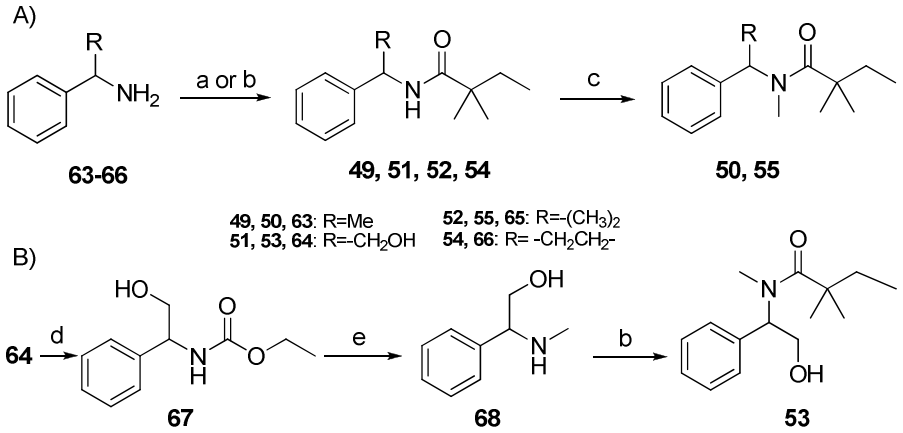


Reagent and conditions: (a) TEA, DCM, rt. (for **49**, **52** and **54**); (b) 2,2-dimethylbutanoyl chloride, aq. $NaHCO_3$, THF/ $H_2O$, 0$^oC$ to rt, 16 h (for **51** and **53**); (c) NaH, DMF, 0$^oC$ to rt, 16 h (for **50** and **55**); (d) ethyl carbonochloridate, aq. $NaHCO_3$, THF/ $H_2O$, 0$^oC$ to rt, 16 h; (e) $LiAH_4$, THF, reflux.

Compounds **56**–**62** were synthesized as outlined in Scheme 4. Nucleophilic displacement of tert-butyl((tert-butoxycarbonyl)oxy)carbamate with fluoro-substituted benzyl bromides (**69**–**75**) afforded intermediate **76**–**82**. Removal of Boc group from **76**–**82** by treatment with TFA in DCM gave hydroxylamine derivatives **83**–**89**, which were treated with 2,2-dimethylbutanoyl chloride to yield the final products **56**–**62**.

**Scheme 4.** Synthesis of compounds **56**–**62**.

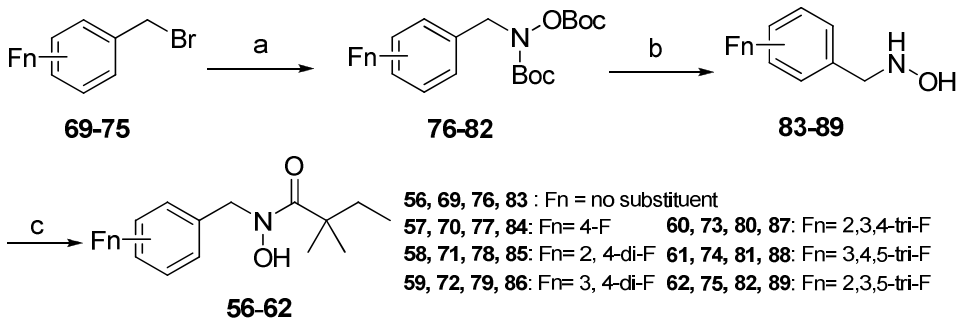

Reagent and conditions: (a) 1 N NaOH, TBAB, DCM; (b) TFA, DCM, rt, 4 h; (c) 2,2-dimethylbutanoyl chloride, aq. $NaHCO_3$, THF, $H_2O$, $0^oC$ to rt, 16 h.

## CONCLUSION

We have described the optimization of an anti-necrosis screening hit into a promising lead, which has novel amide structures and inhibits RIP1 by locking RIP1 kinase in an inactive form as a type III kinase inhibitor. The lead compound — **56** — possesses favorable properties for both a tool compound and a candidate drug: high potency in both human cells and murine cells, high selectivity, high metabolic stability, high efficacy in mice SIRS model, as well as other safety profiles. We anticipate that **56** will be a valuable tool in the further investigations of cell death signaling pathway, and has great potential to be used in clinical trials of inflammatory diseases. Further studies of **56** in different animal models of necrosis-related diseases are in progress.

## EXPERIMENTAL SECTION

**1. Materials and Methods for Chemistry.** All chemical reagents were used as supplied by Sigma-Aldrich, J&K and Alfa Aesar Chemicals. DCM and DMF were distilled from calcium hydride; THF was distilled from sodium/benzophenone ketyl prior to use. $^1$H NMR spectra were recorded on a Varian 400 MHz spectrometer at ambient temperature with $CDCl_3$ as the solvent unless otherwise stated. $^{13}$C NMR spectra were recorded on a Varian 100 MHz spectrometer (with complete proton decoupling) at ambient temperature. Data for $^1$H NMR are reported as follows: chemical shift, multiplicity (s = singlet, d = doublet, t = triplet, q = quartet, m = multiplet), integration and coupling constants. High-resolution mass spectra were obtained using Agilent Technolodies 6540 UHD Accurate-Mass Q-TOF LC/MS. All of the synthesized

compounds were analyzed by UPLC/MS on a Waters Auto Purification LC/MS system (3100 Mass Detector, 2545 Binary Gradient Module, 2767 Sample Manager, and 2998 Photodiode Array (PDA) Detector). The system was equipped with a Waters $C_{18}$ 5μm SunFire separation column(150*4.6 mm), equilibrated with UPLC grade water (solvent A) and UPLC grade acetonitrile (solvent B) with a flow rate of 0.3 mL/min. All of the tested compounds were determined to be ⩾ 95% pure by UPLC.

**2. Synthesis procedure for compounds** 10–62**.**

General synthesis procedure for compounds **10−13**. To a mixture of substituted phenylmethanamine (1 eq, 100 mg) and triethylamine (2 eq) in dry DCM (4 mL) was added 2,2-dimethylbutanoyl chloride (1.2 eq) at $0^{o}$C. The mixture was allowed to stir at room temperature for 2 h. After the amine was consumed as judged by TLC, the mixture was quenched with ice-water, and then extracted with DCM. The organic phase was dried over $Na_2SO_4$, filtered and concentrated. The residue was purified by silica gel chromatography to give the desired products. N-(2-fluorobenzyl)-2,2-dimethylbutanamide (**10**). From (2-fluorophenyl)methanamine and 2,2-dimethylbutanoyl chloride. Colorless oil. Yield, 72.6% . $^{1}$H NMR (400 MHz，$CDCl_3$) δ 7.34-7.30 (m, 1H), 7.25-7.23 (m, 1H), 7.11-7.0 (m, 2H), 6.06 (br, 1H), 4.48 (d, *J* = 6.0 Hz, 2H), 1.55 (q, *J* = 7.6 Hz, 2H), 1.16 (s, 6H), 0.81 (t, *J*=7.6 Hz, 3H). $^{13}$C NMR (100 MHz, $CDCl_3$) δ 177.79, 162.30, 159.85, 130.25 (d, *J* = 4.4 Hz), 129.18 (d, *J* = 8.1 Hz), 125.68 (d, *J* = 14.6 Hz), 124.33 (d, *J* = 3.6 Hz), 115.48, 115.26, 42.50, 37.70, 37.67, 33.94, 24.98, 9.17. HRMS (ESI) $[M+H]^{+}$calad for $C_{13}H_{19}FNO$, 224.1445; found, 224.1464. UPLC purity 98%.

N-(2-bromobenzyl)-2,2-dimethylbutanamide (**11**). From (2-bromophenyl) methanamine and 2,2-dimethylbutanoyl chloride. White solid. Yield, 74%. $^{1}$H NMR (400 MHz, $CDCl_3$) δ 7.55 (dd, *J* = 8.0, 1.2 Hz, 1H), 7.38 (dd, *J* = 7.6, 1.7 Hz, 1H), 7.30 – 7.27 (m, 1H), 7.14 (td, *J* = 7.7, 1.7 Hz,

1H), 4.50 (d, *J* = 5.9 Hz, 2H), 1.55 (q, *J* = 7.5 Hz, 2H), 1.16 (s, 6H), 0.80 (t, *J* = 7.5 Hz, 3H). $^{13}$C NMR (100 MHz, $CDCl_3$) δ 177.75, 137.73, 132.90, 130.75, 129.26, 127.85, 123.87, 44.11, 42.63, 34.06, 25.07, 9.27. HRMS (ESI) $[M+H]^+$ calad for $C_{13}H_{19}BrNO^+$, 284.0645; found, 284.0645. UPLC purity 98%.

N-(3-bromobenzyl)-2,2-dimethylbutanamide (**12**). From (3-bromophenyl) methanamine and 2,2-dimethylbutanoyl chloride. Colorless oil. Yield, 76%. $^1$H NMR (400 MHz, $CDCl_3$) δ 7.41 – 7.36 (m, 2H), 7.21 – 7.15 (m, 2H), 5.90 (s, 1H), 4.40 (d, *J* = 5.8 Hz, 2H), 1.56 (q, *J* = 7.5 Hz, 2H), 1.16 (s, 6H), 0.84 (t, *J* = 7.5 Hz, 3H). $^{13}$C NMR (100 MHz, $CDCl_3$) δ 177.85, 141.27, 130.66, 130.49, 130.31, 126.26, 122.72, 42.95, 42.54, 33.93, 25.06, 9.30. HRMS (ESI) $[M+H]^+$ calad for $C_{13}H_{19}BrNO^+$, 284.0645; found, 284.0651. UPLC purity 98%.

N-benzyl-N,2,2-trimethylbutanamide (**13**). To cold (0$^o$C) a solution of N-benzyl-2,2-dimethylbutanamide (50 mg) in dry DMF (4 mL), sodium hydride (14.6 mg) was added under $N_2$. After the mixture was stirred for 2 h at 0$^o$C, iodomethane (52 mg) was added and the mixture was allowed to warm to room temperature and stirred for 11 h. The mixture was quenched with cold water and extracted with DCM, the combined organic layers was washed with water, brine, dried over $Na_2SO_4$, concentrated and the residue was purified by silica gel column chromatography to give the product as a colorless oil (18.8 mg, 35%). $^1$H NMR (400 MHz, $cdcl_3$) δ 7.40 – 7.21 (m, 5H), 4.65 (s, 2H), 3.00 (s, 3H), 1.70 (q, *J* = 7.5 Hz, 2H), 1.31 (s, 6H), 0.92 (t, *J* = 7.5 Hz, 3H). $^{13}$C NMR (100 MHz, $CDCl_3$) δ 177.14, 128.72, 127.71, 127.34, 53.35, 43.30, 35.99, 33.42, 26.76, 9.91. HRMS (ESI) $[M+H]^+$ calad for $C_{14}H_{22}NO$, 220.1696; found, 220.1696. UPLC purity 97%.

N-(2-fluorobenzyl)-N,2,2-trimethylbutanamide (**14**). N-(2-fluorobenzyl)-2,2-dimethylbutanamide (40 mg) was dissolved in 4 mL of dry DMF, 8.61 mg of NaH was added at

0°C under $N_2$ and stirred for 2 h. Methyl iodide (51 mg) was added and the mixture was allowed to warm to room temperature and stirred for 11 h. The mixture was quenched with cold water and extracted with DCM, the combined organic layers was washed with water, brine, dried over $Na_2SO_4$, concentrated and the residue was purified by silica gel column chromatography to give the product as a light yellow oil (21 mg, 51%). $^1$H NMR(400 MHz，$CDCl_3$) $\delta$ 7.28-7.22 (m, 2H), 7.12-7.01 (m, 2 H), 4.68 (s, 2H), 3.05(s, 3H), 1.65 (q, $J$ = 7.6 Hz, 2H), 1.27(s, 6H), 0.89(t, $J$ = 7.6 Hz, 3H). $^{13}$C NMR (100 MHz, $CDCl_3$) δ 177.13, 162.23, 159.79, 129.67, 128.84, 128.76, 124.78, 124.64, 124.35, 124.31, 46.75, 46.71, 43.17, 36.28, 33.24, 26.53, 9.40. HRMS (ESI) $[M+H]^+$calad for $C_{14}H_{21}FNO$, 238.1602; found, 238.1604. UPLC purity 96%.

N-ethyl-N-(2-fluorobenzyl)-2,2-dimethylbutanamide (**15**). Compound **15** was prepared from N-(2-fluorobenzyl)-2,2-dimethylbutanamide, NaH and iodoethane using the method described in the preparation of compound **14** as a colorless oil in 65% yield. $^1$H NMR (400 MHz, $CDCl_3$): δ 7.26-7.22 (m, 2H), 7.12-7.03 (m, 2H), 4.69 (s, 2H), 3.43 (d, $J$ = 5.2 Hz, 2H), 1.67 (q, $J$ = 7.6 Hz, 2H), 1.26 (s, 6H), 1.17 (t, $J$ =6.8 Hz, 3H), 0.89 (t, $J$ =7.6 Hz, 3H). LC-MS (ESI) $[M+H]^+$ calad for $C_{15}H_{24}FNO$ 252.18; found, 252.21. UPLC purity 96%.

General synthesis procedure for compounds **16**–**36**. A mixture of $K_2CO_3$ (207 mg, 1.5 mmol) and methanamine hydrochloride (202 mg, 3.0 mmol) in 5 mL of MeOH was stirred at rt for 30 min. Then the aromatic aldehyde (248 mg, 2.0 mmol) was added to the mixture and stirred at rt for 1 h. The mixture was cooled to 0°C, and $NaBH_4$ (113.5 mg, 3.0 mmol) was added in portions. The mixture was stirred at 0°C for 1 h and warmed to room temperature and stirred for 2 h. The solid was filtered and washed with EtOAc. The filtrate was evaporated to dryness and the residue was dissolved in EtOAc and was washed with water, brine, dried over $Na_2SO_4$, concentrated. The residue was dissolved in a mixture of dry THF (10 mL) and DIEA (264 mg, 2.05 mmol),

and then 2,2-dimethylbutanoyl chloride (275 mg, 2.05 mmol) was added slowly to the mixture at 0$^{o}$C under nitrogen, stirred at room temperature for 2 h. The reaction was quenched by adding water (15 mL) and extracted with EtOAc (10 mL x 3). The combined organic was washed with 1 M HCl, brine, dried over $Na_2SO_4$, filtered and concentrated. The residue was purified by silica gel column chromatography (PE/EA) to give the corresponding product.

N-(2-chlorobenzyl)-N,2,2-trimethylbutanamide (**16**). From 2-chlorobenzaldehyde (281 mg), methanamine hydrochloride (202 mg) and 2,2-dimethylbutanoyl chloride (275 mg). White solid. Yield, 48%. $^{1}$H NMR (400 MHz, $CDCl_3$) δ7.37-7.35 (m, 1 H), 7.25-7.16 (m, 3 H), 4.74 (s, 2 H), 3.05 (s, 3 H), 1.70 (q, *J* = 7.6 Hz, 2H), 1.28 (s, 6 H), 0.91 (t, *J* = 7.6 Hz, 3 H). $^{13}$C NMR (100 MHz, $CD_3OD$) δ 177.82, 134.54, 129.29, 128.34, 127.72, 126.88, 50.73, 42.97, 35.99, 32.77, 25.53, 8.46. HRMS (ESI) [M+H] $^{+}$calad for $C_{14}H_{21}ClNO$, 254.1306; found, 254.1306. UPLC purity 95%.

N-(3-fluorobenzyl)-N,2,2-trimethylbutanamide (**17**). From 3-fluorobenzaldehyde (124 mg), methanamine hydrochloride (101 mg) and 2,2-dimethylbutanoyl chloride (140 mg). Colorless oil. Yield, 65%. $^{1}$H NMR (400 MHz, $CDCl_3$) *δ* 7.31-7.25 (m, 1 H), 7.01-6.91 (m, 3 H), 4.61 (s, 2 H), 3.01 (s, 3 H), 1.69 (q, *J* = 7.6 Hz，2 H), 1.29 (s, 6 H), 0.90 (t, *J* = 7.6 Hz，3 H). $^{13}$C NMR (100 MHz, $CDCl_3$) δ 177.01, 164.24, 161.79, 140.48, 140.40, 130.08, 130.00, 123.09, 114.19, 113.98, 52.82, 43.12, 36.04, 33.19, 26.50, 9.41. HRMS (ESI) [M+H] $^{+}$calad for $C_{14}H_{21}FNO$, 238.1602; found, 238.1606. UPLC purity 95%.

N-(3-chlorobenzyl)-N,2,2-trimethylbutanamide (**18**). From 3-chlorobenzaldehyde (140 mg), methanamine hydrochloride (101 mg) and 2,2-dimethylbutanoyl chloride(140 mg). White solid. Yield, 48%. $^{1}$H NMR (400 MHz, $CDCl_3$) δ7.26-7.20 (m, 3 H), 7.12-7.10 (m, 1 H), 4.59 (s, 2 H),

3.01 (s, 3 H), 1.68 (q, $J$ = 7.6 Hz，2H), 1.28 (s, 6 H), 0.90 (t, $J$ = 7.6 Hz，3H). HRMS (ESI) $[M+H]^+$ calad for $C_{14}H_{21}ClNO$, 254.1306; found, 254.1302. UPLC purity 96%.

N-(3-bromobenzyl)-N,2,2-trimethylbutanamide (**19**). From 3-bromobenzaldehyde (185 mg), methanamine hydrochloride (101mg) and 2,2-dimethylbutanoyl chloride (140 mg). White solid. Yield, 48%. $^1$H NMR ($CDCl_3$, 400 MHz): δ 7 7.36-7.40 (m, 2 H), 7.16-7.22 (m, 2 H), 4.59 (s, 2 H), 3.01 (s, 3 H), 1.69 (q, 2 H, J = 7.6 Hz), 1.29 (s, 6 H), 0.90 (t, 3 H, J = 7.6 Hz). $^{13}$C NMR (100 MHz, $CD_3OD$) δ 179.24, 141.66, 131.57, 131.45, 131.41, 127.41, 123.59, 53.74, 49.64, 49.43, 49.21, 49.00, 48.79, 48.57, 48.36, 44.32, 36.90, 34.06, 26.97, 9.78. HRMS (ESI) $[M+H]^+$calad for $C_{14}H_{21}BrNO_2$, 298.0796; found, 298.0802, 300.0782. UPLC purity 96%.

N-(3-hydroxybenzyl)-N,2,2-trimethylbutanamide (**20**). From 3-hydroxybenzaldehyde (122 mg), methanamine hydrochloride (101 mg) and 2,2-dimethylbutanoyl chloride (140 mg). White solid. Yield, 33%. $^1$H NMR ($CDCl_3$, 400 MHz):δ7.17 (t, 1 H, J = 7.6 Hz), 6.71-6.79 (m, 3 H), 4.58 (s, 2 H), 2.98 (s, 3 H), 1.68 (q, 2 H, J = 7.6 Hz), 1.29 (s, 6 H), 0.90 (t, 3 H, J = 7.6 Hz). $^{13}$C NMR (100 MHz, $CDCl_3$) δ 177.67, 157.44, 129.74, 114.90, 77.48, 77.16, 76.84, 53.42, 43.34, 36.18, 33.30, 26.72, 9.59. LC-MS (ESI) $[M+H]^+$ calad for $C_{14}H_{22}NO_2$, 236.1640; found, 236.1641. UPLC purity 96%.

N-(4-fluorobenzyl)-N,2,2-trimethylbutanamide (**21**). From 4-fluorobenzaldehyde (248 mg), methanamine hydrochloride (202 mg) and 2,2-dimethylbutanoyl chloride (275 mg). Colorless oil. Yield, 54%. $^1$H NMR (400 MHz, $CDCl_3$): δ 7.21 – 7.12 (m, 2H), 6.98-6.93 (m, 2H), 4.54 (s, 2H), 2.95 (s, 3H), 1.64 (q, $J$ = 7.5 Hz, 2H), 1.24 (s, 6H), 0.84 (t, $J$ = 7.5 Hz, 3H). $^{13}$C NMR (100 MHz, $CDCl_3$) δ 176.77, 163.12, 160.68, 133.44, 133.41, 129.22, 129.14, 115.33, 115.12, 77.32, 77.00, 76.68, 52.39, 42.97, 35.66, 33.08, 26.39, 9.26. LC-MS (ESI) $[M+H]^+$calad for: $C_{14}H_{21}FNO$, 238.1602; found, 238.1598. UPLC purity 96%.

N-(2,3-difluorobenzyl)-N,2,2-trimethylbutanamide (**22**). From 2,3-difluorobenzaldehyde (284 mg), methanamine hydrochloride (202 mg) and 2,2-dimethylbutanoyl chloride (275 mg). Colorless oil. Yield, 56%. $^{1}$H NMR (400 MHz, $CDCl_3$) δ 7.11 – 6.94 (m, 3H), 4.66 (s, 2H), 3.06 (s, 3H), 1.66 (q, *J* = 7.5 Hz, 2H), 1.25 (s, 6H), 0.85 (t, *J* = 7.5 Hz, 3H). $^{13}$C NMR (100 MHz, $CDCl_3$) δ 177.07, 151.64, 151.51, 150.17, 150.04, 149.17, 149.04, 147.71, 147.58, 127.33, 127.21, 124.17, 124.12, 124.10, 124.06, 115.98, 115.81, 46.49, 43.07, 36.36, 33.08, 9.28. HRMS (ESI) [M+H] $^{+}$calad for: $C_{14}H_{20}F_2NO$, 256.1507; found, 256.1511. UPLC purity 97%.

N-(2,4-difluorobenzyl)-N,2,2-trimethylbutanamide (**23**). From 2,4-difluorobenzaldehyde (284 mg), methanamine hydrochloride (202 mg) and 2,2-dimethylbutanoyl chloride (275 mg). Colorless oil. Yield, 50%. $^{1}$H NMR(400 MHz, $CDCl_3$) δ 7.25-7.31 (m, 1H), 6.76-6.86 (m, 2H), 4.60 (s, 2H), 3.06 (s, 3H), 1.65 (q, *J*= 7.6 Hz，2H), 1.26 (s, 6 H), 0.85 (t, *J*= 7.6 Hz，3H ). $^{13}$C NMR (100 MHz, $CDCl_3$) δ 177.23, 163.46, 163.35, 162.32,162.20, 161.00, 160.88, 159.85, 159.73, 131.10, 120.89, 120.86, 120.74, 120.71, 111.68, 11.50, 111.47,103.93, 103.68, 103.42, 46.43, 46.40, 43.23, 36.40, 33.23, 26.58, 9.46. HRMS (ESI) [M+H] $^{+}$calad for: $C_{14}H_{20}F_2NO$, 256.1507; found, 256.1522. UPLC purity 97%.

N-(2,5-difluorobenzyl)-N,2,2-trimethylbutanamide (**24**). From 2,5- difluorobenzaldehyde (284 mg), methanamine hydrochloride (202 mg) and 2,2-dimethylbutanoyl chloride (275 mg). White solid. Yield, 59%. $^{1}$H NMR (400 MHz, $CDCl_3$) δ7.02-6.89 (m, 3H), 4.63 (s, 2H), 3.08 (s, 3H), 1.68 (q, *J* = 7.6 Hz，2H), 1.28 (s, 6 H), 0.88 (t, *J* = 7.6 Hz，3H). $^{13}$C NMR (100 MHz, $CD_3OD$) δ 179.27, 161.46, 161.44, 159.53, 159.50, 159.07, 159.04, 127.99, 127.91, 127.81, 127.74, 117.83, 117.7, 117.58, 117.49, 116.55, 116.46, 116.31, 116.22, 48.18, 48.14, 44.33, 37.36, 34.00, 26.85, 9.69. HRMS (ESI) [M+H] $^{+}$calad for: $C_{14}H_{20}F_2NO$, 256.1507; found, 256.1509. UPLC purity 96%.

N,2,2-trimethyl-N-(2,3,5-trifluorobenzyl)butanamide (**25**). From 2,3,5-trifluorobenzaldehyde (320 mg), methanamine hydrochloride (202 mg) and 2,2-dimethylbutanoylchloride (275 mg). Colorless oil. Yield, 50%. $^{1}$H NMR (400 MHz, $CDCl_3$) δ 6.85-6.75 (m, 2 H), 4.64 (s, 2 H), 3.11 (s, 3 H), 1.68 (q, $J$ = 7.6 Hz，2H), 1.28 (s, 6 H), 0.88 (t, $J$ = 7.6 Hz，3H). LC-MS (ESI) $[M+H]^+$ calad for $C_{14}H_{19}F_3NO$, 274.14; found 274.16. $^{13}$C NMR (100 MHz, $CDCl_3$) δ 177.23, 128.45, 128.36, 128.31, 128.23, 110.71, 110.48, 104.48, 104.21, 104.00, 46.66, 43.11, 36.63, 33.06, 26.34, 9.32. HRMS (ESI) $[M^+H]$ $^+$calad for $C_{14}H_{19}F_3NO$, 274.1413; found, 274.1412. UPLC purity 96%.

N,2,2-trimethyl-N-(2,4,6-trifluorobenzyl)butanamide (**26**). From 2,4,6-trifluorobenzaldehydhyde (320 mg), methanamine hydrochloride (202 mg) and 2,2-dimethylbutanoylchloride (275 mg). Colorless oil. Yield, 62%.$^{1}$H NMR (400 MHz, $CDCl_3$): δ 6.61-6.69 (m, 2 H), 4.64 (s, 2 H), 3.06 (s, 3 H), 1.64 (q, 2 H, J = 7.6 Hz ), 1.24 (s, 6 H), 0.82 (t, 3 H, J = 7.6 Hz). $^{13}$C NMR (100 MHz, $CDCl_3$) δ 176.56, 163.46, 163.40,163.31, 163.29, 160.99, 160.91, 160.83, 160.80, 160.76, 160.65, 110.10, 110.06, 109.91, 109.87, 109.72, 109.68, 100.56, 100.54, 100.31, 100.28, 100.25, 100.02, 100.00, 43.28, 41.42, 36.08, 33.15, 26.53, 9.29. HRMS (ESI) $[M^+H]$ $^+$calad for$C_{14}H_{19}F_3NO$, 274.1413; found, 274.1416. UPLC purity 95%.

N,2,2-trimethyl-N-(pyridin-4-ylmethyl)butanamide (**27**). From isonicotinaldehyde (214 mg), methanamine hydrochloride (202mg) and 2,2-dimethylbutanoyl chloride (289 mg). Light yellow oil. Yield, 86%. $^{1}$H NMR ($CDCl_3$, 400 MHz): δ 8.55 (brs, 2 H), 7.13 (d, 2 H, J = 5.6 Hz), 4.59 (s, 2 H), 3.05 (s, 3 H), 1.69 (q, 2 H, J = 7.6 Hz), 1.28 (s, 6 H), 0.89 (t, 3 H, J = 7.6 Hz). $^{13}$C NMR (100 MHz, $CDCl_3$) δ 177.26, 149.99, 147.14, 122.46, 52.64, 43.19, 36.60, 33.22, 26.49, 9.50. HRMS (ESI) $[M+H]$ $^+$calad for $C_{13}H_{21}N_2O$, 221.1648; found, 221.1642. UPLC purity 97%.

N,2,2-trimethyl-N-(pyridin-3-ylmethyl)butanamide (**28**). From nicotinaldehyde (214 mg), methanamine hydrochloride (202 mg) and 2,2-dimethylbutanoyl chloride (289 mg). Light yellow oil. Yield, 86%. $^{1}$H NMR ($CDCl_3$, 400 MHz): δ8.48-8.51 (m, 2 H), 7.58-7.61 (m, 1 H), 7.24-7.27 (m, 1 H), 4.59 (s, 2 H), 3.03 (s, 3 H), 1.66 (q, 2 H, J = 7.6 Hz), 1.27 (s, 6 H), 0.86 (t, 3 H, J = 7.6 Hz). $^{13}$C NMR (100 MHz, $CDCl_3$) δ 177.11, 149.21, 148.79, 135.70, 133.51, 123.70, 50.97, 43.16, 36.16, 33.21, 26.53, 9.46. HRMS (ESI) [M+H] $^{+}$calad for $C_{13}H_{21}N_2O$, 221.1648; found, 221.1643. UPLC purity 97%.

N-((3-fluoropyridin-4-yl)methyl)-N,2,2-trimethylbutanamide (**29**). From 3-fluoroisonicotinaldehyde (125 mg), methanamine hydrochloride (101 mg) and 2,2-dimethylbutanoyl chloride (134 mg). White solid. Yield, 78%. $^{1}$H NMR ($CDCl_3$, 400 MHz): δ8.41 (d, 1 H, J = 1.6 Hz), 8.35 (d, 1 H, J = 4.8 Hz ), 7.18 (dd, 1 H, J = 6.0, 5.2 Hz), 4.65 (s, 2 H), 3.12 (s, 3 H), 1.68 (q, 2 H, J = 7.6 Hz), 1.27 (s, 6 H), 0.87 (t, 3 H, J = 7.6 Hz ). $^{13}$C NMR (100 MHz, $CDCl_3$) δ 177.35, 146.00 (d, *J* = 5.1 Hz), 137.99, 137.75, 133.74 (d, *J* = 12.5 Hz), 123.46, 46.64 (d, *J* = 3.8 Hz), 43.18, 36.99, 33.13, 26.39, 9.42. HRMS (ESI) [M+H] $^{+}$calad for $C_{13}H_{20}FN_2O$, 239.1554; found, 239.1536. UPLC purity 97%.

N,2,2-trimethyl-N-(thiophen-2-ylmethyl)butanamide (**30**). From thiophene-2-carbaldehyde (224 mg), methanamine hydrochloride (202 mg) and 2,2-dimethylbutanoyl chloride (119 mg). Yellow oil. Yield, 62%. $^{1}$H NMR ($CDCl_3$, 400 MHz): δ7.21 (dd, 1 H, J = 4.8, 1.6 Hz), 6.92-6.95 (m, 2 H), 4.71 (s, 2 H), 3.05 (s, 3 H), 1.66 (q, 2H, J = 7.6 Hz), 1.27 (s, 6 H), 0.86 (t, 3 H, J = 7.6 Hz). $^{13}$C NMR (100 MHz, $CDCl_3$) δ 176.75, 140.58, 126.43, 126.41, 125.48, 48.56, 43.16, 35.77, 33.35, 26.59, 24.63, 9.53. HRMS (ESI) [M+H] $^{+}$calad for $C_{12}H_{20}NOS$, 226.1260; found, 226.1269. UPLC purity 96%.

N,2,2-trimethyl-N-((3-methylthiophen-2-yl)methyl) butanamide (**31**). From 3-methylthiophene-2-carbaldehyde (200 mg), methanamine hydrochloride (161 mg) and 2,2-dimethylbutanoylchloride (218 mg). Yellow oil. Yield, 42%. $^{1}$H NMR ($CDCl_3$, 400 MHz): δ7.11 (d, 1 H, J = 5.2 Hz), 6.78 (d, 1 H, J = 5.2 Hz), 4.68 (s, 2 H), 3.03 (s, 3 H), 2.23 (s, 3 H), 1.67 (q, 2 H, J = 7.6 Hz), 1.27 (s, 6 H), 0.89 (t, 3 H, J = 7.6 Hz). $^{13}$C NMR (100 MHz, $CDCl_3$) δ 176.65, 134.95, 134.10, 129.76, 123.50, 46.12, 43.24, 35.70, 33.40, 26.62, 13.83, 9.55. HRMS (ESI) [M+H] $^{+}$calad for $C_{13}H_{22}NOS$, 240.1417; found, 240.1405. UPLC purity 96%.

N,2,2-trimethyl-N-((5-methylthiophen-2-yl)methyl)butanamide (**32**). From 5-methylthiophene-2-carbaldehyde (200 mg), methanamine hydrochloride (161 mg) and 2,2-dimethylbutanoylchloride (218 mg). Gray solid. Yield, 42%. $^{1}$H NMR ($CDCl_3$, 400 MHz): δ6.72 (d, 1 H, J = 3.2 Hz), 6.56-6.57 (m, 1 H), 4.62 (s, 2 H), 3.03 (s, 3 H), 2.43 (d, 3 H, J = 1.2 Hz), 1.661 (q, 2 H, J = 7.6 Hz), 1.269 (s, 6 H), 0.877 (t, 3 H, J = 7.6 Hz). HRMS (ESI) [M+H] $^{+}$calad for $C_{13}H_{22}NOS$, 240.1417; found, 240.1414. UPLC purity 98%.

N-((4,5-dimethylthiophen-2-yl)methyl)-N,2,2-trimethylbutanamide (**33**). From 4,5-dimethylthiophene-2-carbaldehyde, methanamine hydrochloride and 2,2-dimethylbutanoyl chloride. Light yellow oil. Yield, 36%. $^{1}$H NMR: ($CDCl_3$, 400 MHz): δ6.61 (s, 1 H), 4.58 (s, 2 H), 3.03 (s, 3 H), 2.28 (s, 3 H), 2.07 (s, 3 H), 1.66 (q, 2 H, J = 7.6 Hz), 1.27 (s, 6 H), 0.88 (t, 3 H, J = 7.6 Hz). $^{13}$C NMR (100 MHz, $CDCl_3$) δ 176.72, 135.51, 132.76, 132.28, 129.41, 48.70, 43.19, 35.66, 33.41, 26.64, 13.63, 13.19, 9.60. HRMS (ESI) [M+H] $^{+}$calcd for $C_{14}H_{24}NOS$, 254.1573; found, 254.1569. UPLC purity 98%.

N-(furan-2-ylmethyl)-N,2,2-trimethylbutanamide (**34**). From furan-2-carbaldehyde (500 mg), methanamine hydrochloride (527 mg) and 2,2-dimethylbutanoylchloride (714 mg). Light yellow solid.Yield, 26% $^{1}$H NMR($CDCl_3$,400 MHz): 7.34-7.35 (m, 1 H), 6.31-6.33 (m, 1 H), 6.21-6.22

(m, 1 H), 4.57 (s, 2H), 3.06 (s, 3 H), 1.63 (q, 2 H, J=7.6 Hz ), 1.27(s, 6 H), 0.85 (t, 3 H, J=7.6 Hz) LC-MS (ESI) $[M+H]^+$calad for $C_{12}H_{20}NO_2$, 210.2; found, 210.3. UPLC purity 95%.

N,2,2-trimethyl-N-((2-methylthiazol-5-yl)methyl) butanamide (**35**). From 2-methylthiazole-5-carbaldehyde (60 mg), methanamine hydrochloride (48 mg) and 2,2-dimethylbutanoylchloride (74 mg). Gray solid. Yield, 23%. $^1$H NMR ($CDCl_3$, 400 MHz): δ7.50 (s, 1 H), 4.59 (s, 2 H), 3.07 (s, 3 H), 2.67 (s, 3 H), 1.64 (q, 2 H, J = 7.6 Hz), 1.25 (s, 6 H), 0.84 (t, 3 H, J = 7.6 Hz). HRMS (ESI) $[M+H]^+$calad for $C_{12}H_{21}N_2OS$, 241.1369; found, 241.1374. UPLC purity 95%.

N,2,2-trimethyl-N-((1-methyl-1H-pyrazol-3-yl)methyl) butanamide (**36**). From N,1-dimethyl-1H-pyrazol-3-amine (30 mg), and 2,2-dimethylbutanoylchloride(48 mg). Gray solid. Yield, 23%. $^1$H NMR ($CDCl_3$, 400 MHz): δ7.26 (d, 1 H, J= 4.0 Hz), 6.12 (d, 1 H, J = 4.0 Hz), 4.57 (s, 2 H), 3.85 (s, 3 H), 3.01 (s, 3 H), 1.65 (q, 2 H, J = 7.6 Hz), 1.26 (s, 6 H), 0.85 (t, 3 H, J = 7.6 Hz). HRMS (ESI) $[M+H]^+$calad for $C_{12}H_{22}N_3O$, 224.1757; found, 224.1736. UPLC purity 95%.

General synthesis procedure of compounds **37**–**44**. A mixture of $K_2CO_3$ (323 mg, 2.34 mmol) and methanamine hydrochloride (316 mg, 4.68 mmol) in 10 mL of MeOH was stirred at RT for 30 min. Then 2,3,5-trifluorobenzaldehyde (500 mg, 3.12 mmol) was added to the mixture and stirred at room temperature for 1 h. The mixture was cooled to 0$^o$C, and $NaBH_4$ (178 mg, 4.68 mmol) was added in portions. The mixture was stirred at 0$^o$C for 1 h and warmed to room temperature and stirred for 2 h. The solid was filtered and washed with EtOAc. The filtrate was evaporated to dryness and the residue was dissolved in EtOAc and was washed with water, brine, dried over $Na_2SO_4$. Filtered and evaporated to dryness to yield N-methyl-1-(2,3,5-trifluorophenyl) methanamine, which was used for next step without further purification.

The above methylamine compounds (25 mg, 0.142 mmol) and the corresponding aliphatic acid (0.142 mmol, 1 eq) were dissolved in 1 mL of DMF. HATU (0.21 mmol, 1.5 eq ) and DIEA

(0.282 mmol, 2 eq) were added and the mixture was stirred at room temperature for 12 h, evaporated to dryness and purified by preparative TLC (petroleum ether/ethyl acetate, 6:1) to give desired products.

N-methyl-N-(2,3,5-trifluorobenzyl) pivalamide (**37**). From N-methyl-1-(2,3,5-trifluorophenyl) methanamine and pivaloyl acid. Colorless oil. Yield, 54%. $^1$H NMR (400 MHz, $CDCl_3$) δ 6.88 – 6.78 (m, 1H), 6.75 – 6.68 (m, 1H), 4.65 (s, 2H), 3.11 (s, 3H), 1.33 (s, 9H). LC-MS (ESI) $[M+H]^+$calad for $C_{13}H_{17}F_3NO$, 260.1257; found, 260.1258. UPLC purity 95%.

2-methoxy-N,2-dimethyl-N-(2,3,5-trifluorobenzyl) propanamide (**38**). From N-methyl-1-(2,3,5-trifluorophenyl) methanamine and 2-methoxy-2-methyl propanoic acid. Colorless oil. Yield, 13%. $^1$H NMR (400 MHz, $CDCl_3$) δ 6.90-6.82 (m, 2H), 4.49 (s, 2H), 3.27 (s, 3H), 3.22 (s, 3H), 1.48 (s, 6H). HRMS (ESI) $[M+H]^+$calad for $C_{13}H_{17}F_3NO_2$, 276.1206; found, 276.1204. UPLC purity 95%.

3-hydroxy-N,2,2-trimethyl-N-(2,3,5-trifluorobenzyl)propanamide (**39**). From N-methyl-1-(2,3,5-trifluorophenyl) methanamine and 3-hydroxy-2,2-dimethylpropanoic acid . Colorless oil. Yield, 34%. $^1$H NMR: ($CDCl_3$, 400 MHz): δ 6.82 (m, 2 H), 4.52 (s, 2 H), 3.57 (s, 2 H), 3.06 (s, 3 H), 1.32 (s, 6 H). HRMS (ESI) $[M+H]^+$ calad for $C_{13}H_{17}F_3NO_2$,276.1206; found 276.1192. UPLC purity 95%.

N,1-dimethyl-N-(2,3,5-trifluorobenzyl) cyclopropanecarboxamide (**40**). From N-methyl-1-(2,3,5-trifluorophenyl) methanamine and 1-methylcyclopropanecarboxylic acid. White solid. Yield, 35% . $^1$H NMR(400 MHz, $CD_3OD$) δ 7.07 – 6.91 (m, 2H), 4.53 (s, 2H), 3.13 (s, 3H), 1.33, 0.94 (q, $J$ = 4.5 Hz, 2H), 0.65 (q, $J$ = 4.6 Hz, 2H). $^{13}$C NMR (100 MHz, $CD_3OD$) δ 177.04, 153.78, 151.29, 141.26, 138.78, 135.84, 112.89, 51.19, 35.76, 21.51, 13.71. HRMS (ESI) $[M+H]^+$ calad for $C_{13}H_{15}F_3NO$, 258.1100; found, 258.1102. UPLC purity 97%.

N-methyl-N-(2,3,5-trifluorobenzyl) cyclobutanecarboxamide (**41**). From cyclobutanecarboxylic acid and N-methyl-1-(2,3,5-trifluorophenyl) methanamine. Light yellow oil. Yield, 29.2%. $^{1}$H NMR: ($CDCl_3$, 400 MHz): δ6.76-6.86 (m, 2H), 4.61(s, 2H), 3.29-3.33 (m, 1H), 2.89 (s, 3H), 2.32-2.41 (m, 2H), 2.17-2.22 (m, 2H), 1.86-1.99 (m, 2H). $^{13}$C NMR (100 MHz, $CDCl_3$) δ 175.19, 111.29, 111.05, 104.79, 104.58, 104.58, 104.52, 104.31, 44.48, 37.54, 34.91, 25.12, 18.00. HRMS (ESI) $[M+H]^+$ calad for $C_{13}H_{15}F_3NO$, 258.1100; found, 258.1090. UPLC purity 97%.

N-methyl-N-(2,3,5-trifluorobenzyl)-1-(trifluoromethyl)cyclobutanecarboxamide (**42**). From 1-(trifluoromethyl) cyclobutanecarboxylic acid (30 mg) and N-methyl-1-(2,3,5-trifluorophenyl) methanamine (31 mg). Yellow oil. Yield, 25.9%. $^{1}$H NMR: ($CDCl_3$, 400 MHz): δ 6.80-6.89 (m, 1H), 6.74-6.77 (m, 1H), 4.66(s, 2H), 2.92 (s, 3H), 2.68-2.77(m, 2H), 2.52-2.58(m, 2H), 2.08-2.16(m, 1H), 1.83-1.87(m, 1H). $^{13}$C NMR (100 MHz, $CD_3OD$) δ 171.12, 130.19, 127.40, 111.74, 111.49, 105.92, 105.71, 105.64, 105.43, 53.06, 52.80, 46.86, 36.77, 28.84, 28.82, 16.30. HRMS (ESI) $[M+H]^+$ calad for $C_{14}H_{13}F_6NO$, 326.0974; found 326.0978. UPLC purity 97%.

N-methyl-N-(2,3,5-trifluorobenzyl)-1-(trifluoromethyl)cyclopentanecarboxamide (**43**). From 1-(trifluoromethyl) cyclopentanecarboxylic acid (30 mg) and N-methyl-1-(2,3,5-trifluorophenyl) methanamine (29 mg). Light yellow oil. Yield, 26.9%. $^{1}$H NMR: ($CDCl_3$, 400 MHz): δ 6.79-6.85 (m, 1H), 6.65-6.69 (m, 1H), 4.65 (s, 2H), 3.07(s, 3H), 2.38-2.44 (m, 2H), 2.15-2.21(m, 2H), 1.59-1.74 (m, 4H). LC-MS (ESI) $[M+H]^+$ calad for $C_{15}H_{15}F_6NO$, 340.1131; found, 340.1130. UPLC purity 96%.

N,1-dimethyl-N-(2,3,5-trifluorobenzyl)cyclohexanecarboxamide (**44**). From N-methyl-1-(2,3,5-trifluorophenyl) methanamine and 1-methylcyclohexanecarboxylic acid. Yellow oil. Yield, 19.5% .$^{1}$H NMR: ($CDCl_3$, 400 MHz) δ (ppm) 6.80-6.82 (m, 1H), 6.72-6.76 (m, 1H), 4.65 (s, 2H), 3.10 (s, 3H), 2.06-2.11 (m, 2H), 1.36-1.54 (m, 8H), 1.27 (s, 3H). $^{13}$C NMR (100 MHz,

$CDCl_3$) δ 177.64, 128.63, 110.64, 110.42, 104.60, 104.39, 104.33, 104.12, 46.97, 43.13, 37.23, 37.01, 26.05, 24.22, 23.22. HRMS (ESI) $[M+H]^+$ calad for $C_{16}H_{21}F_3NO$, 300.1564; found, 300.1545. UPLC purity 96%.

Isopropyl-1,3-dimethyl-3-(2,3,5-trifluorobenzyl)urea (**45**). To a solution of triphosgene (84.8 mg) in dichloromethane (4 mL) was added N-methylpropan-2-amine (20.86 mg) at 0°C under nitrogen. The mixture was stirred at 0 °C for 4 h. Then the solvent was removed, and a solution of N-(2,3,5-trifluorobenzyl)methanamine (30 mg) in dichloromethane (2 mL) was added. The mixture was stirred at 35°C for overnight, diluted with water. The aqueous layer was extracted with EtOAc (5 mL x 3). The combined organic layers were washed with saturated $NaHCO_3$ and brine, dried with $Na_2SO_4$, filtered and evaporated to dryness. The residue was purified by column chromatography to give compound **45** as a light yellow solid (9.8 mg, 20.8%). $^1H$ NMR: ($CDCl_3$, 400 MHz): δ6.80-6.87 (m, 2H), 4.38 (s, 2H), 4.00-4.11 (m, 1H), 2.75 (s, 3H), 2.67 (s, 3H), 1.10 (d, 6H, J = 6.4 Hz). HRMS (ESI) $[M+H]^+$ calad for $C_{13}H_{18}F_3N_2O$, 275.1366; found, 275.1351. UPLC purity 97%.

1,1-diisopropyl-3-methyl-3-(2,3,5-trifluorobenzyl)urea (**46**). The titled compound **46** was prepared in 19.3% yield as a light yellow solid from triphosgene (84.8 mg), diisopropylamine (26.86 mg) and N-methyl-1-(2,3,5-trifluorophenyl)methanamine (30 mg) according to the procedure described in the preparation of compound **45**. $^1H$ NMR: ($CDCl_3$, 400 MHz): δ6.79-6.82 (m, 2 H), 4.30 (s, 2 H), 3.58-3.62 (m, 2 H), 2.68 (s, 3 H), 1.26 (d, 12 H, J = 6.4 Hz).LC-MS (ESI) [M+H]+ calad for $C_{15}H_{21}F_3N_2O$, 303.2; found, 303.4. UPLC purity 97%.

N,2-dimethyl-N-(2,3,5-trifluorobenzyl)piperidine-1-carboxamide (**47**). The titled compound **47** was prepared in 9.7% yield as a light yellow solid from triphosgene (84.8mg), 2-methylpiperidine (28.3mg) and N-methyl-1-(2,3,5-trifluorophenyl)methanamine (30mg)

according to the procedure outlined for compound **45**. $^1$H NMR: ($CDCl_3$, 400 MHz): δ 6.78-6.84 (m, 2 H), 4.43 (d, *J* = 16 Hz, 1 H), 4.34 (d, *J* = 16 Hz, 1 H), 3.90-3.93 (m, 1 H), 3.32-3.36 (m, 1 H), 2.95-3.02 (m, 1 H), 2.76 (s, 3 H), 1.44-1.68 (m, 6 H), 1.18 (d, *J* = 4 Hz, 3 H). LC-MS (ESI) $[M+H]^+$ calad for $C_{15}H_{20}F_3N_2O$, 301.1; found, 301.3. UPLC purity 95%.

N,2,6-trimethyl-N-(2,3,5-trifluorobenzyl)piperidine-1-carboxamide (**48**). The titled compound **48** was prepared in 14.5% yield as a light yellow solid from triphosgene (84.8 mg), 2,6-dimethylpiperidine (32.28 mg) and N-methyl-1-(2,3,5-trifluorophenyl)methanamine (30 mg) according to the procedure outlined for compound 45 . $^1$H NMR: ($CDCl_3$, 400 MHz): δ 6.80-6.90 (m, 2H), 4.61 (s, 2H,), 3.18-3.23 (m, 2H), 2.97 (s, 3H), 1.70-1.75 (m, 1H), 1.59-1.65 (m, 2H), 1.32-1.45 (m, 1H), 1.22-1.39 (m, 2H), 1.12 (d, *J* = 6.4 Hz, 6H). HRMS (ESI) [M+H]+ calad for $C_{16}H_{22}F_3N_2O$, 315.1673; found, 315.1651. UPLC purity 97%.

2,2-dimethyl-N-(1-phenylethyl)butanamide (**49**). 1-phenylethanamine (1 g, 8.26 mmol) and Triethylamine (0.918 g, 9.09 mmol) were dissolved in 20 mL of dry $CH_2Cl_2$. 2,2-dimethylbutanoyl chloride (1.223 g, 9.09 mmol) in 2 mL of $CH_2Cl_2$ was added slowly to the solution at 0$^o$C under nitrogen. The mixture was stirred at room temperature for 2 h, diluted with $CH_2Cl_2$ and water. The organic layer was washed with saturated $NaHCO_3$, brine, dried with $Na_2SO_4$ and concentrated. The residue was purified by chromatography to give compound **49** (1.35 g, 74.6%) as an white solid. $^1$H NMR(400 MHz, $CDCl_3$) δ 7.34-7.26 (m, 5H), 5.77 (brs, 1H), 5.10-5.17 (m, 1H), 1.55 (q, *J* = 8Hz, 2H), 1.49 (d,*J*=4Hz, 3H), 1.15 (s, 6H), 0.82 (t, *J*= 8Hz, 3H). $^{13}$C NMR (100 MHz, $CDCl_3$) δ 176.78, 143.59, 128.69, 127.29, 126.16, 48.52, 42.32, 34.00, 25.02, 21.78, 9.24. HRMS (ESI) $[M+H]^+$calad for $C_{14}H_{22}NO$, 220.1696; found, 220.1707. UPLC purity 97%.

N,2,2-trimethyl-N-(1-phenylethyl)butanamide (**50**). To a solution of compound **49** (50 mg) in dry THF (1 mL) sodium hydride (13.7 mg) was added under nitrogen at 0°C. The mixture was stirred at 0°C for 30 minutes, then iodomethane (38.9 mg) was added. The mixture was stirred at room temperature for 2 h and quenched with cold water and extracted with $CH_2Cl_2$. The combined organic layer were washed with $H_2O$, dried with $Na_2SO_4$ and concentrated. The residue was purified by chromatography to give compound **50** (8 mg, 15%) as a white solid $^1$H NMR ($CDCl_3$, 400 MHz): δ7.32-7.35 (m, 2H), 7.22-7.27 (m, 3H), 5.62-6.30 (m, 1H), 2.70 (s, 3H), 1.68 (q, 2H, J = 7.6 Hz), 1.51 (d, 3H, J = 6.0 Hz), 1.30 (s, 3H), 1.29 (s, 3H), 0.91 (t, 3H, J = 7.6 Hz). LC-MS (ESI) $[M+H]^+$calad for $C_{15}H_{24}NO$, 234.1852; found, 234.1828. UPLC purity 97%.

N-(2-hydroxy-1-phenylethyl)-2,2-dimethylbutanamide (**51**). 2-amino-2-phenylethanol (50 mg, 0.365 mmol) and $NaHCO_3$ (91.9 mg, 1.094 mmol) were dissolved in 2 mL of THF/$H_2O$ (v/v, 1/1). 2,2-dimethylbutanoylchloride (43 mg, 0.398 mmol) was added slowly to the solution at 0°C under nitrogen. The mixture was stirred at room temperature for 16 h, and extracted with EtOAc (15 mL x 3). The combined organic layers were washed with brine, dried with $Na_2SO_4$. Filtered and evaporated to dryness. The residue was purified by column chromatography to give compound **51** as a white solid (75 mg, 78.2%). $^1$H NMR: (400 MHz, $CDCl_3$) δ7.40-7.36 (m, 2H), 7.33-7.28 (m, 3H), 6.27 (brs, 1H), 5.07 (dd, *J* = 5.6, 10.8 Hz, 1H), 3.92-3.88 (m, 2 H), 2.72 (brs, 1 H), 1.58 (q, *J* = 7.6 Hz, 2 H), 1.20 (s, 3 H), 1.19 (s, 3 H), 0.87 (t, *J* = 7.6 Hz, 3H). $^{13}$C NMR (100 MHz, $CDCl_3$) δ 178.69, 139.33, 129.09, 128.02, 126.70, 67.22, 56.09, 42.67, 34.08, 25.13, 25.06, 9.35. HRMS (ESI) $[M+H]^+$ calad for $C_{15}H_{22}NO_2$, 236.1645; found, 236.1646. UPLC purity 97%.

2,2-dimethyl-N-(2-phenylpropan-2-yl)butanamide (**52**). The titled compound **52** was prepared in 64.4% yield as a white solid from 2-phenylpropan-2-amine (135 mg) and 2,2-dimethylbutanoyl chloride (147.5 mg) according to the procedure outlined for compound **49**. $^1$H NMR: (400 MHz, $CDCl_3$) δ 7.30-7.39 (m, 4H), 7.20-7.24 (m, 1H), 5.83 (brs, 1H), 1.70 (s, 6H), 1.53 (q, *J* = 7.6 Hz, 2H), 1.15 (s, 6H), 0.86 (t, *J* = 7.6 Hz, 3H) LC-MS (ESI) [M+H]+ calad for $C_{15}H_{24}NO$, 233.2; found, 233.3. UPLC purity 97%.

N-(2-hydroxy-1-phenylethyl)-N,2,2-trimethylbutanamide (**53**). The titled compound **53** was prepared in 9.8% yield as a yellow oil from 2-(methylamino)-2-phenylethanol (50 mg) and 2,2-dimethylbutanoyl chloride (48 mg) according to the procedure outlined for compound **51**. $^1$H NMR: (MeOD, 400 MHz) δ7.43-7.44 (m, 3H), 7.28-7.38 (m, 2H), 4.29-4.38 (m, 2H), 5.88 (m, 1H), 2.43 (s, 3H), 1.528 (q, *J* = 7.6 Hz, 2H), 1.11 (s, 6H), 0.75 (t, *J* = 7.6 Hz, 3H). HRMS (ESI) $[M+H]^+$ calad for $C_{15}H_{24}NO_2$, 250.1796; found, 250.1778. UPLC purity 97%.

2,2-dimethyl-N-(1-phenylcyclopropyl)butanamide (**54**). The titled compound **54** was prepared in 96% yield as a white solid from 1-phenylcyclopropanamine (106 mg) and 2,2-dimethylbutanoyl chloride (160 mg) according to the procedure outlined for compound **49**. $^1$H NMR($CDCl_3$, 400 MHz): δ7.22-7.29 (m, 4H), 7.15-7.19 (m, 1H), 6.25 (brs, 1H), 1.54 (q, *J* = 7.6 Hz, 2H), 1.24-1.29 (m, 2H), 1.18-1.22 (m, 2H), 1.16 (s, 6H), 0.81 (t, 3H, J = 7.6 Hz). $^{13}$C NMR (100 MHz, $CDCl_3$) δ 177.90, 142.79, 128.40, 126.33, 125.58, 42.39, 35.00, 34.06, 25.12, 18.00, 9.26. HRMS (ESI) $[M+H]^+$calad for $C_{15}H_{21}NO$, 232.1696; found, 232.1672. UPLC purity 97%.

N,2,2-trimethyl-N-(2-phenylpropan-2-yl)butanamide (**55**). The titled compound **55** was prepared in 30% yield as a white solid from compound **52** (90 mg), sodium hydride (32 mg) and iodomethane (85.2 mg) according to the procedure outlined for compound **50**. $^1$H NMR ($CDCl_3$, 400 MHz) δ 7.23-7.27 (m, 4H), 7.11-7.17 (m, 1H), 3.03 (s, 3H), 1.62 (q, *J* = 7.6 Hz, 2H), 1.61 (s,

6H), 1.19 (s, 6H), 0.82 (t, $J$ = 7.6 Hz, 3H). HRMS (ESI) $[M+H]^+$calad for $C_{16}H_{24}NO$, 246.1852; found, 246.1829. UPLC purity 95%.

N-benzyl-N-hydroxy-2,2-dimethylbutanamide (**56**).

Tert-butyl(tert-butoxycarbonyl)oxycarbamate (247 mg) and (bromomethyl)benzene (181 mg) were dissolved in $CH_2Cl_2$ (20 mL). The mixture was added 1 M NaOH (1.1 mL) and tetrabutylammonium bromide (17 mg), and stirred at room temperature for overnight. The resulting mixture was washed with water and dried with $Na_2SO_4$, concentrated in vacuo and purification by silica gel chromatography to give tert-butyl benzyl((tert-butoxycarbonyl)oxy)carbamate (308 mg, 90%). $^1$H NMR($CDCl_3$, 400 MHz): δ 7.32-7.41 (m, 5H), 4.50(s, 2H), 1.48(s, 9H), 1.46(s, 9H).

The above intermediate was dissolved in $CH_2Cl_2$ (6 mL), TFA (3 mL) was added at 0$^o$C. The mixture was stirred at room temperature for 4 h and concentrated to give N-benzylhydroxylamine (200 mg) as a TFA salt, which was used without further purification.

The above intermediate was dissolved in THF (7 mL) and water (7 mL) and 2.4 mL of saturated aqueous $NaHCO_3$ was added. The mixture was stirred at room temperature for 30 min, then cooled to 0$^o$C, 2,2-dimethylbutanoylchloride (128 mg) was added and stirred for overnight. The mixture was extracted with EtOAc, washed with brine, dried ($Na_2SO4$), and concentrated in vacuo. Purification by silica gel chromatography to give compound **56** as a white solid (101 mg, total yield 43.3%). $^1$H NMR (400 MHz, $CDCl_3$) δ 7.34-7.37 (m, 2H), 7.31-7.33 (m, 3H), 4.89 (s, 2H), 1.69 (q, $J$ = 7.6Hz, 2H), 1.26 (s, 6H), 0.86 (t, $J$ = 7.6 Hz, 6H). $^{13}$C NMR (100 MHz, $CD_3OD$) δ 178.93, 138.29, 129.38, 129.31, 128.41, 106.43, 54.74, 44.24, 33.03, 25.75, 9.80. HRMS (ESI) $[M+H]^+$ calad for $C_{13}H_{20}NO_2$, 222.1489; found, 222.1487. UPLC purity 98%.

N-(4-fluorobenzyl)-N-hydroxy-2,2-dimethylbutanamide (**57**). The titled compound **57** was prepared in 52% yield as a light yellow solid from tert-butyl (tert-butoxycarbonyl)oxycarbamate (247 mg), 1-(bromomethyl)-4-fluorobenzene (200 mg) and 2,2-dimethylbutanoylchloride (121 mg) according to the procedure outlined for compound **56**. $^{1}$H NMR (400 MHz, $CDCl_3$) δ 7.27-7.31 (m, 2H), 7.02-7.06 (m, 2H), 4.85 (s, 2H), 1.68 (q, *J* = 7.6 Hz, 2H), 1.26 (s, 6H), 0.84 (t, *J* = 7.6 Hz, 3H). $^{13}$C NMR (100 MHz, $CDCl_3$) δ 179.00, 164.86, 162.44, 134.35, 134.32, 131.37, 131.29, 116.10, 115.89, 54.03, 44.22, 32.99, 25.72, 9.78. HRMS (ESI) $[M+H]^+$ calad for $C_{13}H_{18}FNO_2$, 240.1397; found, 240.1393. UPLC purity 96%.

N-(2,4-difluorobenzyl)-N-hydroxy-2,2-dimethylbutanamide (**58**). The titled compound **58** was prepared in 53% yield as a light yellow solid from tert-butyl (tert-butoxycarbonyl)oxycarbamate (225 mg), 1-(bromomethyl)-2,4-difluorobenzene (200 mg) and 2,2-dimethylbutanoylchloride (121 mg) according to the procedure outlined for compound **56**. $^{1}$H NMR ($CDCl_3$, 400 MHz): δ 7.32-7.38 (m, 1H), 6.80-6.90 (m, 2H), 4.90 (s, 2H), 1.68 (q, *J* = 7.6 Hz, 2H), 1.25 (s, 6H), 0.84 (t, *J* = 7.6 Hz, 3H). $^{13}$C NMR (100 MHz, $CD_3OD$) δ 179.19, 165.08 (d, *J* = 11.9 Hz), 163.80 (d, *J* = 12.3 Hz), 162.63 (d, *J* = 11.8 Hz), 161.33 (d, *J* = 11.8 Hz), 132.79 (dd, *J* = 9.8, 5.7 Hz), 121.28 (dd, *J* = 15.1, 3.7 Hz), 112.16 (dd, *J* = 21.5, 3.8 Hz), 104.67, 104.41, 104.15, 47.44 (d, *J* = 3.3 Hz), 44.28, 32.97, 25.69, 9.77. HRMS (ESI) $[M+H]^+$ calad for $C_{13}H_{18}F_2NO_2$, 258.1300; found, 258.1300. UPLC purity 96%.

N-(3,4-difluorobenzyl)-N-hydroxy-2,2-dimethylbutanamide (**59**). The titled compound **59** was prepared in 58% yield as a light yellow solid from tert-butyl (tert-butoxycarbonyl)oxycarbamate (225 mg), 4-(bromomethyl)-1,2-difluorobenzene (200 mg) and 2,2-dimethylbutanoylchloride (121 mg) according to the procedure outlined for compound **56**. $^{1}$H NMR ($CDCl_3$, 400 MHz): δ7.10-7.17 (m, 2H), 7.02-7.06 (m, 1H), 4.81 (s, 2H), 1.68 (q, *J* = 7.6 Hz, 2H), 1.25 (s, 6H), 0.84

(t, $J$ = 7.6 Hz, 3H). $^{13}$C NMR (100 MHz, $CD_3OD$) δ 179.20, 152.57 (d, $J$ = 12.8 Hz), 152.16 (d, $J$ = 12.5 Hz), 150.12 (d, $J$ = 12.8 Hz), 149.72 (d, $J$ = 12.7 Hz), 135.89 (dd, $J$ = 5.1, 4.0 Hz), 125.86 (dd, $J$ = 6.5, 3.6 Hz), 118.16 (dd, $J$ = 17.5, 13.9 Hz), 53.92, 44.23, 32.95, 25.66, 9.77. HRMS (ESI) $[M+H]^+$ calad for $C_{13}H_{18}F_2NO_2$, 258.1300; found, 258.1308. UPLC purity 96%.

N-hydroxy-2,2-dimethyl-N-(2,3,4-trifluorobenzyl)butanamide (**60**). The titled compound **60** was prepared in 52% yield as a light yellow solid from tert-butyl (tert-butoxycarbonyl)oxycarbamate (104 mg), 1-(bromomethyl)-2,3,4-trifluorobenzene (100 mg) and 2,2-dimethylbutanoylchloride (54 mg) according to the procedure outlined for compound **56**. $^1$H NMR ($CDCl_3$, 400 MHz): δ 7.08-7.14 (m, 1H), 6.93-7.00 (m, 1H), 4.92 (s, 2H), 1.68 (q, $J$ = 7.6 Hz, 2H), 1.25 (s, 6H), 0.84 (t, $J$ = 7.6 Hz, 3H). $^{13}$C NMR (100 MHz, $CD_3OD$) δ 179.24, 153.07 (dd, $J$ = 10.2, 2.9 Hz), 152.40 (dd, $J$ = 10.3, 3.6 Hz), 150.59 (dd, $J$ = 9.9, 2.9 Hz), 149.92 (dd, $J$ = 9.9, 3.4 Hz), 142.13, 139.66, 125.67 (dt, $J$ = 8.7, 4.5 Hz), 123.19 (dd, $J$ = 12.4, 3.7 Hz), 113.11 (dd, $J$ = 17.6, 3.9 Hz), 47.45, 44.29, 32.94, 25.63, 9.74. HRMS (ESI) $[M+H]^+$ calad for $C_{13}H_{17}F_3NO_2$, 276.1206; found, 276.1208. UPLC purity 96%.

N-hydroxy-2,2-dimethyl-N-(3,4,5-trifluorobenzyl)butanamide (**61**). The titled compound **61** was prepared in 55% yield as a light yellow solid from tert-butyl(tert-butoxycarbonyl)oxycarbamate (104 mg), 5-(bromomethyl)-1,2,3-trifluorobenzene (100 mg) and 2,2-dimethylbutanoylchloride (54 mg) according to the procedure outlined for compound **56**. $^1$H NMR(400 MHz, $CDCl_3$) δ 6.92−7.00 (m, 2H), 4.79 (s, 2H), 1.68 (q, $J$ = 7.6 Hz, 2H), 1.26 (s, 6H), 0.85 (t, $J$ = 7.6 Hz, 3H).$^{13}$C NMR (100 MHz, $CD_3OD$) δ 179.00, 152.09, 152.05, 151.99, 151.95, 149.62, 149.58, 149.52, 149.49, 139.91, 137.51, 134.14, 112.13, 112.08, 111.97, 111.92, 52.52, 42.81, 31.49, 24.16, 8.31. HRMS (ESI) $[M+H]^+$ calad for $C_{13}H_{17}F_3NO_2$, 276.1206; found, 276.1208. UPLC purity 96%.

N-hydroxy-2,2-dimethyl-N-(2,3,5-trifluorobenzyl)butanamide (**62**). The titled compound **62** was prepared in 72.7% yield as a light yellow solid from tert-butyl(tert-butoxycarbonyl)oxycarbamate (104 mg), 5-(bromomethyl)-2,3,5-trifluorobenzene (100 mg) and 2,2-dimethylbutanoylchloride (54 mg) according to the procedure outlined for compound **56**. $^1$H NMR (400 MHz, DMSO-$d_6$): δ 9.80 (s, 1H), 7.41-7.48 (m, 1H), 6.91-6.96 (m, 1H), 4.74 (s, 2H), 1.64 (q, $J$ = 7.6 Hz, 2H), 1.13 (s, 6H), 0.72 (t, $J$ = 7.6 Hz, 3H). LC-MS (ESI) $[M+H]^+$ calad for $C_{13}H_{17}F_3NO_2$, 276.1; found, 276.1. UPLC purity 95%.

**3. Materials for Biological Experiments.**

Recombinant mouse TNFα was purchased from Genscript (Nanjing, China). Antibodies of human RIP1, human RIP3, and actin were purchased from Cell Signaling Technologies. Anti-RIP3 phosphorylated Serine227 antibody was purchased from Abcam. Recombinant RIP1 and RIP3 protein were purchased from SignalChem. The ADP-Glo™ kinase assay kit and CellTiter-Glo® kit were purchased from Promega. The kits for mouse IL-1ß and IL-6 determination were purchased from PerkinElmer. Kits for CK-MB, LDH, creatinine, BUN, ALT, and AST were purchased from Nanjing Jiancheng Bioengineering Institute. Recombinant human IDO was purchased from Sino Biological Inc. (Beijing, China). Human HT-29 cells and mouse L929 cells were purchased from ATCC (Manassas, VA, USA) and maintained in McCoy's 5A culture medium (Invitrogen) and DMEM (Invitrogen) respectively. Each medium was supplemented with 10% fetal bovine serum (Invitrogen) and 100-unit/mL penicillin/streptomycin (Hyclone). Human and mouse liver microsomes were purchased from BD Biosciences. C57BL/6J mice matched for gender and age were purchased from Vitalriver. All experiments on mice were conducted according to institutional and national animal regulations. Animal protocols were

approved by the ethics committee of national institute of biological sciences. Mice were used at the age of 6–8 weeks.

**4. *In vitro* kinase activity assay and IDO enzyme activity assay.** The RIP1 kinase assay was performed in white 384-well plate. The assay buffer contained 25 mM HEPES (pH7.2), 20 mM $MgCl_2$, 12.5 mM $MnCl_2$, 5 mM EGTA, 2 mM EDTA, 12.5 mM β-glycerol phosphate and 2 mM DTT. RIP1 was first incubated with compounds or DMSO control for 15 min, then ATP/MBP substrate mixture was added to initiate the reaction. The final concentration of ATP was 50 μM, and MBP 20 μM. After 90 min reaction at room temperature, the ADP-Glo reagent and detection solution were added following the technical manual. The RIP3 kinase assay conditions were almost identical to that of RIP1 assay, except the assay buffer contained 5 mM $MgCl_2$ instead of 20 mM $MgCl_2$ and 12.5 mM $MnCl_2$. The luminescence was measured on PerkinElmer Enspire. The IDO enzymatic assay was conducted according to the protocols previously described8 with some modifications. Briefly, the reaction mixture contained 50 mM MES buffer (pH 6.5), 20 mM ascorbic acid (prepared in 0.405 M Tris, pH 8.0), 2250 U/mL catalase, 10 μM methylene blue, 200 μM L-tryptophan (L-Trp), 100 nM purified recombinant IDO, and 200 μM compounds or DMSO control per reaction. The reaction was carried out at 37 $^{o}$C for 3 h. The yellow color generated from the reaction with kynurenine was measured at 321 nm using Enspire plate reader.

**5. Cell necrosis assay.** Cell necrosis assay was performed in 96-well cell culture plate. 3,000 cells were plated in each well and cultured at 37$^{o}$C overnight. HT-29 cells were treated with 20 ng/mL TNFα/100 nM Smac Mimetics/20 μM z-VAD-FMK and compounds for 24 h. L929 cells were treated with 20 ng/mL TNFα/20 μM z-VAD-FMK and compounds for 6 h. The cell survival ratio was determined using the Cell Titer-Glo Luminescent Cell Viability Assay kit.

**6. Data analysis.** Data were analyzed using GraphPad Prism (GraphPad Software, Inc., San Diego, CA, USA). The curves were fitted using a non-linear regression model with a sigmoidal dose response.

**7. Western-Blot analysis.** Cell pellet was collected and re-suspended with lysis buffer (20 mM Tris-HCl, pH 7.4, 150 mM NaCl, 10% glycerol, 1% Triton X-100, 1 mM $Na_3VO_4$, 25 mM ß-glycerol-phosphate, 0.1mM PMSF, complete protease inhibitor cocktail and phosphatase inhibitor cocktail (Roche). The re-suspended cell pellet was incubated on ice for 30 min and centrifuged at 13,000 g for 10 min. The supernatants were collected for Western-blot analysis.

**8. Molecular Docking.** The X-ray crystal structure of RIP1 kinase domain (PDB: 4ITH) was used for docking studies. Before docking simulation, ligands and protein were prepared with the standard protocol using MOE 2015.10 software, including the addition of hydrogens, the assignment of bond order, assessment of the correct protonation state. All docking calculations were performed using default settings.

**9. Compounds stability test in liver microsome assays.** Compounds were incubated with human or mouse liver microsomes and NADPH in 0.05 M Phosphate buffer (pH=7.4) at 37°C for 0-60 min. The reaction was quenched and the amount of the remaining compound was analyzed using LC-MS/MS.

**10. Phamacokinetics study in mice.** Following intraveneous (IV), intraperitoneal (IP), or oral administration (PO) of **56** to C57BL/6 mice (n = 3), blood was sampled through eye puncture at various time points. Compound concentrations in the plasma samples were analyzed by LC-MS/MS. Pharmacokinetic parameters were determined from individual animal data using non-compartmental analysis in phoenix 64 (winNonlin 6.3).

**11. TNFα-induced mice SIRS model.** C57BL/6 mice were used at the age of 6–8 weeks with the average body weight of 20 g, and were grouped randomly (n = 6 ~10). Mouse TNFα was diluted in endotoxin-free PBS and injected intravenously in a volume of 0.2 mL. Different doses of **56** were IP injected before (-17 min) and after (once every 12 h) mTNFα injection unless otherwise specified, while an equal amount of solvent was injected to control mice. Mice mortality was continuously monitored every 30 min until 60 h after TNFα administration. For cytokines, and biomarkers determination, blood samples were collected 12 h, and 24 h after TNFα injection respectively.

**12. Histology.** For histology analysis, mice were sacrificed at 24 h after TNFα injection. Organs were separated immediately and fixed in 10% neutral buffered formalin for 24 h. The fixed tissues were dehydrated in ethanol, cleared in xylene, and embedded in paraffin blocks. Five-micrometre sections were cut and mounted on adhesion microscope slides, and then stained with haematoxylin and eosin (H&E). The stained sections were analyzed by Beijing Lawke Health Laboratory Center and the investigators were blinded to allocation when the histology experiments were performed.

## ASSOCIATED CONTENT

### Supporting Information.

Figure s1 ~ Figure s5. Table s1 ~ Table s3. $^{1}H$ and $^{13}C$ NMR spectra of compounds. (WORD) Molecular Formula Strings. (CSV)

This material is available free of charge via the Internet at http://pubs.acs.org.

## AUTHOR INFORMATION

### Corresponding Author

* E-mail: zhangzhiyuan@nibs.ac.cn, Phone: +86-10-80726688-8575; wangxiaodong@nibs.ac.cn, Phone: +86-10-80726688-8396.

**Present Addresses**

[「]Institute of Biochemistry and Cell Biology, Shanghai Institutes for Biological Sciences, Chinese Academy of Sciences, 320 Yue-yang Road, Shanghai 200031, China. [#]Cyrus Tang Hematology Center, Soochow University, 199 Ren'ai Rd. Suzhou, Jiangsu 215123, China. [I]Peking Union Medical College, Chinese Academy of Medical Sciences, China.

**Author Contributions**

All authors have given approval to the final version of the manuscript. [‡]These authors contributed equally to this work. Zhiyuan Zhang and Xiaodong Wang conceived the project; Zhiyuan Zhang and Yaning Su designed, Yaning Su and Hanying Ruan synthesized more than 80% of the compounds; Yan Ren designed and conducted the biochemical experiments; Liming Sun and Sisi Li determined the compounds potency using cell necrosis assay; Sudan He screened the compounds library and found the initial hit compound; Xiaoguang Lei designed and Daohong Liao synthesized compound **2**, **3**, and 5; Xiao Liu and Yongfen Ma prepared compounds formulation, tested the compounds stability and pharmacokinetic parameters; Yan Ren together with Lingjun Meng and Chunyan Liu designed and conducted mice model experiments; Yan Ren and Yaning Su drafted the manuscript.

**Funding Sources**

This work was supported by National Major Scientific and Technological Special Project for “Significant New Drugs Development” during the Twelfth Five-year Plan Period 2013ZX0950910 from the Chinese Ministry of Science and Technology.

## Notes

The authors declare no competing financial interest

## ACKNOWLEDGMENT

We thank Yong Yu and Pengfei Liu for the help of several compounds synthesis.

## ABBREVIATIONS

SIRS, systemic inflammatory response syndrome; RIP1, Receptor-interacting protein 1; RIP3, Receptor-interacting protein 3; MLKL, Mixed lineage kinase domain-like protein; Nec1, Necrostatin-1; IDO, indoleamine 2,3-dioxygenase; NSA, Necrosulfonamide; TNFα, tumor necrosis factor alpha; Smac, second mitochondrial-derived activator of caspases; z-VAD-FMK, Z-Val-Ala-Asp-(OMe)-Fluoromethyl Ketone; TSZ, TNFα/Smac mimetic/z-VAD; SAR, structure-activity relationship; Compd, compound; Asp, aspartic acid; Met, methionine; Phe, phenylalanine; PK, pharmacokinetic; IP, intraperitoneal injection; PO, oral administration; IV, intravenous administration; BW, body weight; mIL-6, mouse interleukin-6; mIL-1ß, mouse interleukin-1ß; PALS, periarteral lymphatic sheath; LDH, lactate dehydrogenase; CK, creatine kinase; AST, aspartate aminotransferase; BUN, blood urea nitrogen.

## REFERENCES

1. Murdoch, W.; Wilken, C.; Young, D. Sequence of apoptosis and inflammatory necrosis within the formative ovulatory site of sheep follicles. *J. Reprod. Fertil.* **1999**, *117*, 325-329.

2. Jäättelä, M.; Tschopp, J. Caspase-independent cell death in T lymphocytes. *Nat. Immunol.* **2003**, *4*, 416-423.

3. Pasparakis, M.; Vandenabeele, P. Necroptosis and its role in inflammation. *Nature* **2015**, *517*, 311–320.

4. Linkermann, A.; Bräsen, J. H.; De Zen, F.; Weinlich, R.; Schwendener, R. A.; Green, D. R.; Kunzendorf, U.; Krautwald, S. Dichotomy between RIP1-and RIP3-mediated necroptosis in tumor necrosis factor-α-induced shock. *Mol. Med.* **2012**, *18*, 577-586.

5. Linkermann, A.; Bräsen, J. H.; Himmerkus, N.; Liu, S.; Huber, T. B.; Kunzendorf, U.; Krautwald, S. Rip1 (receptor-interacting protein kinase 1) mediates necroptosis and contributes to renal ischemia/reperfusion injury. *Kidney Int*. **2012**, *81*, 751-761.

6. Duprez, L.; Takahashi, N.; Van Hauwermeiren, F.; Vandendriessche, B.; Goossens, V.; Berghe, T. V.; Declercq, W.; Libert, C.; Cauwels, A.; Vandenabeele, P. RIP kinase-dependent necrosis drives lethal systemic inflammatory response syndrome. *Immunity* **2011**, *35*, 908-918.

7. Degterev, A.; Huang, Z.; Boyce, M.; Li, Y.; Jagtap, P.; Mizushima, N.; Cuny, G. D.; Mitchison, T. J.; Moskowitz, M. A.; Yuan, J. Chemical inhibitor of nonapoptotic cell death with therapeutic potential for ischemic brain injury. *Nat. Chem. Biol.* **2005**, *1*, 112-119.

8. Takahashi, N.; Duprez, L.; Grootjans, S.; Cauwels, A.; Nerinckx, W.; DuHadaway, J.; Goossens, V.; Roelandt, R.; Van Hauwermeiren, F.; Libert, C. Necrostatin-1 analogues: critical issues on the specificity, activity and *in vivo* use in experimental disease models. *Cell Death Dis.* **2012**, *3*, e437.

9. Lin, J.; Li, H.; Yang, M.; Ren, J.; Huang, Z.; Han, F.; Huang, J.; Ma, J.; Zhang, D.; Zhang, Z. A role of RIP3-mediated macrophage necrosis in atherosclerosis development. *Cell Rep.* **2013**, *3*, 200-210.

10. Cauwels, A.; Janssen, B.; Waeytens, A.; Cuvelier, C.; Brouckaert, P. Caspase inhibition causes hyperacute tumor necrosis factor–induced shock via oxidative stress and phospholipase A2. *Nat. Immunol.* **2003**, *4*, 387-393.

11. He, S.; Wang, L.; Miao, L.; Wang, T.; Du, F.; Zhao, L.; Wang, X. Receptor interacting protein kinase-3 determines cellular necrotic response to TNF-α. *Cell* **2009**, *137*, 1100-1111.

12. Degterev, A.; Hitomi, J.; Germscheid, M.; Ch'en, I. L.; Korkina, O.; Teng, X.; Abbott, D.; Cuny, G. D.; Yuan, C.; Wagner, G. Identification of RIP1 kinase as a specific cellular target of necrostatins. *Nat. Chem. Biol.* **2008**, *4*, 313-321.

13. Sun, L.; Wang, H.; Wang, Z.; He, S.; Chen, S.; Liao, D.; Wang, L.; Yan, J.; Liu, W.; Lei, X.; Wang, X. Mixed lineage kinase domain-like protein mediates necrosis signaling downstream of RIP3 kinase. *Cell* **2012**, *148*, 213-227.

14. Teng, X.; Degterev, A.; Jagtap, P.; Xing, X.; Choi, S.; Denu, R.; Yuan, J.; Cuny, G. D. Structure–activity relationship study of novel necroptosis inhibitors. *Bioorg. Med. Chem. Lett.* **2005**, *15*, 5039-5044.

15. Najjar, M.; Suebsuwong, C.; Ray, S. S.; Thapa, R. J.; Maki, J. L.; Nogusa, S.; Shah, S.; Saleh, D.; Gough, P. J.; Bertin, J. Structure guided design of potent and selective ponatinib-based hybrid inhibitors for RIPK1. *Cell Rep.* **2015**, *10*, 1850-1860.

16. Harris, P. A.; King, B. W.; Bandyopadhyay, D.; Berger, S. B.; Campobasso, N.; Capriotti, C. A.; Cox, J. A.; Dare, L.; Dong, X.; Finger, J. N.; Grady, L. C. ; Hoffman, S. J. ; Jeong, J. U.; Kang, J.; Kasparcova, V.; Lakdawala, A. S.; Lehr, R.; McNulty, D. E.; Nagilla, R.; Ouellette, M. T.; Pao, C. S. Rendina, A. R.; Schaeffer, M. C.; Summerfield, J. D.; Swift, B. A.; Totoritis, R. D.; Ward, P.; Zhang, A. ; Zhang, D.; Marquis, R. W.; Bertin, J.; Gough, P. J. DNA-encoded library screening identifies benzo[b][1,4]oxazepin-4-ones as highly potent and monoselective receptor interacting protein 1 kinase inhibitors. *J. Med. Chem*. **2016**, *59*, 2163-2178.

17. Berger, S.; Harris, P.; Nagilla, R.; Kasparcova, V.; Hoffman, S.; Swift, B.; Dare, L.; Schaeffer, M.; Capriotti, C.; Ouellette, M. Characterization of GSK'963: a structurally distinct, potent and selective inhibitor of RIP1 kinase. *Cell Death Discov*. **2015**, *1*, 15009.

18. Harris, P.; Bandyopadhyay, D., Berger, S.; Campobasso, N.; Capriotti, C.; Cox, J.; Dare, L.; Finger, J.; Hoffman, S.; Kahler, K.; Lehr, R.; Lich, J.; Nagilla, R.; Nolte, R.; Ouellette, M.; Pao, C.; Schaeffer, M.; Smallwood, A.; Sun, H.; Swift, B.; Totoritis, R.; Ward, P.; Marquis, R.; Bertin, J.; and Gough, P. Discovery of small molecule RIP1 kinase inhibitors for the treatment of pathologies associated with necroptosis. *ACS Med. Chem. Lett.* **2013**, *4*, 1238−1243.

19. Mandal, P.; Berger, S. B.; Pillay, S.; Moriwaki, K.; Huang, C.; Guo, H.; Lich, J. D.; Finger, J.; Kasparcova, V.; Votta, B. RIP3 induces apoptosis independent of pronecrotic kinase activity. *Mol. Cell* **2014**, *56*, 481-495.

20. Xie, T.; Peng, W.; Liu, Y.; Yan, C.; Maki, J.; Degterev, A.; Yuan, J. ; Shi, Y. Structural basis of RIP1 inhibition by necrostatins. *Structure* **2013**, *21*, 493-499.

21. Degterev, A.; Maki, J.; Yuan, J. Activity and specificity of necrostatin-1, small-molecule inhibitor of RIP1 kinase. *Cell Death Differ.* **2013**, *20*, 366.

22. Vandenabeele, P.; Grootjans, S.; Callewaert, N.; Takahashi, N. Necrostatin-1 blocks both RIPK1 and IDO: consequences for the study of cell death in experimental disease models. *Cell Death Differ.* **2013**, *20*, 185-187.

## Table of Contents Graphic and Synopsis

A highly potent and selective RIP1 inhibitor — compound **56** with favorable pharmacokinetic profile was developed as a potential drug candidate for inflammatory diseases. In a mice model of systemic inflammatory response syndrome (SIRS), **56** could efficiently decrease TNFα-induced mice mortality and multi-organ damage.